



UNIVERSITY *of the*  
WESTERN CAPE

**SYNTHESIS AND CHARACTERIZATION OF BINARY PALLADIUM  
BASED ELECTROCATALYSTS TOWARDS ALCOHOL OXIDATION  
FOR FUEL CELL APPLICATION**

By

Lutho Attwell Klaas

Dissertation in fulfillment of the requirement for the degree

UNIVERSITY *of the*  
**MASTERS**  
WESTERN CAPE

in

Chemical Science

FACULTY OF SCIENCE

of the

UNIVERSITY OF THE WESTERN CAPE

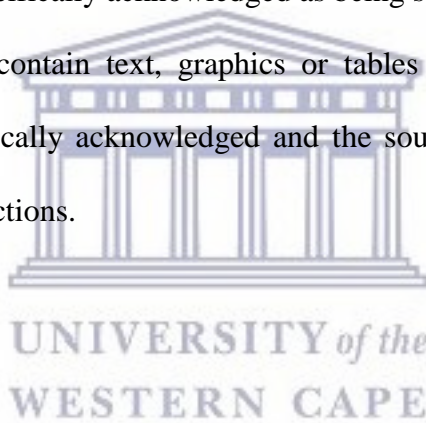
Supervisor: Dr Lindiwe Khotseng

Co-supervisor: Dr Mmalewane Modibedi

**Declaration**

I Lutho Attwell Klaas declare that:

1. The research reported in this thesis, except where otherwise indicated is my original research.
2. This thesis has not been submitted for any other degree or examination at any other university.
3. This thesis does not contain any other person’s data, pictures, graphs or any other information unless specifically acknowledged as being sourced from other persons.
4. This thesis does not contain text, graphics or tables copied and pasted from the internet, unless specifically acknowledged and the source being detail in the thesis and in the reference sections.



\_\_\_\_\_ on this \_\_\_\_ day of \_\_\_\_\_  
(Candidate)

\_\_\_\_\_ on this \_\_\_\_ day of \_\_\_\_\_  
(Supervisor)

\_\_\_\_\_ on this \_\_\_\_ day of \_\_\_\_\_  
(Co-supervisor)

## **Dedication**

This work is dedicated to my loving family. The support you have shown me throughout my studies, not only for this degree but throughout my schooling career is immensely appreciated. Mom and dad, I wouldn't have had the will and discipline to finish this work if it weren't for your teachings. A special dedication goes to my late brother Ntando Klaas, losing you made me realize how short life is, and to never let fear stop me from pursuing my dreams. It is also dedicated to every African kid with a dream.



## Presentations and manuscripts

### Conference presentations

- ❖ **Lutho Klaas, Lindiwe Khotseng, Mmalewane Modibedi: Synthesis and characterization of binary Pd electrocatalysts towards alcohol oxidation for fuel cell application. Poster presentation at the 1<sup>st</sup> Africa Energy Materials Conference, CSIR International Convention Centre, Pretoria. 28 March 2017.**



UNIVERSITY *of the*  
WESTERN CAPE

## Acknowledgements

I would like to express my appreciation and gratitude to the following people and organisations for their contribution towards the success of this work:

- ❖ First and for most I would like to thank the Lord Almighty for giving me the strength to persevere through it all.
- ❖ My supervisor, Dr Khotseng for her guidance and patience during the course of the research work.
- ❖ My co-supervisor Dr Modibedi, thank you so much.
- ❖ The University of the Western Cape, Chemistry Department and the National Research Fund (NRF) and Eskon for their financial support.
- ❖ Fellow postgraduate students within the department and friends for their support.
- ❖ My loving family for their understanding, patience and support.



## **Abstract**

The anode catalyst is one of the important parts of the direct alcohol fuel cell (DAFC); it is responsible for the alcohol oxidation reaction (AOR) takes place at the anode side. Pd has been reported to have good alcohol oxidation reactions and good stability in alkaline solution. Better stability and activity has been reported for Pd alloyed catalysts when compared to Pd. Choosing a suitable alcohol also has an effect on the activity and stability of the catalyst. This study investigates the best catalyst with better AOR and the best stability and also looks at the better alcohol to use between glycerol and ethanol for the five in-house catalysts (20% Pd, PdNi, PdNiO, PdMn<sub>3</sub>O<sub>4</sub> and PdMn<sub>3</sub>O<sub>4</sub>NiO on multi walled carbon nanotubes) using cyclic voltammetry (CV), linear sweep voltammetry (LSV), electrochemical impedance spectrometry (EIS) and chronoamperometry. HR-TEM and XRD techniques were used to determine the particle size and average particle size, respectively while EDS used to determine elemental composition and ICP was used to determine catalyst loading.

It was observed from LSV that PdNiO was the most active catalyst for both ethanol and glycerol oxidation, and it was the most stable in ethanol while PdMn<sub>3</sub>O<sub>4</sub> proved to be the most stable catalyst in glycerol observed using chronoamperometry. The best alcohol in this study was reported to be glycerol having given the highest current densities for all the in-house catalysts compared to ethanol observed using LSV. From XRD and HR-TEM studies, particle sizes were in the range of 0.97 and 2.69 nm for XRD 3.44 and 7.20 nm for HR-TEM with a little agglomeration for PdMn<sub>3</sub>O<sub>4</sub> and PdMn<sub>3</sub>O<sub>4</sub>NiO.

**Table of contents**

Declaration.....i

Dedication.....ii

Presentation and manuscripts.....iii

Acknowledgement.....iv

Abstract .....v

Table of contents.....vi

List of figures.....ix

List of tables.....xiv

List of abbreviations.....xv

Chapter: Introduction.....1

    1. Introduction.....1

        1.1 Background .....1

        1.2 Overview of fuel cells.....6

        1.3 Rational of research project.....9

        1.4 Aims and objectives.....9

        1.5 Thesis outline.....10

        1.6 References.....12

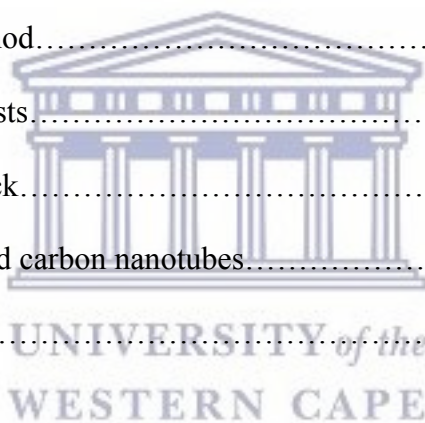
Chapter 2: literature review.....14

    2. Introduction.....14

        2.1 Direct alcohol fuel cells.....14



2.2 Catalysts .....	15
2.2.1 Catalysts used in fuel cells.....	16
2.2.2 Palladium a catalyst for fuel cells.....	16
2.2.3 Palladium binary catalyst for fuel cells.....	17
2.3 Preparation methods for fuel cell catalyst.....	18
2.3.1 Sulphite complex route.....	18
2.3.2 Impregnation method.....	18
2.3.3 Bönneiman method.....	19
2.3.4 Microemulsion method.....	19
2.3.5 Vapour phase method.....	19
2.3.6 Polyol method.....	20
2.4 Supports for catalysts.....	21
2.4.1 Carbon black.....	21
2.4.2 Multi walled carbon nanotubes.....	21
2.5 References .....	23
Chapter 3: Experimental.....	28
3. Introduction.....	28
3.1 Chemicals.....	28
3.2 Methodology.....	29
3.2.1 Pre-treatment of carbon nanotubes.....	29
3.2.2 Preparation of Pd/CNT.....	29
3.2.2.1 Preparation of Pd/CNT.....	29
3.2.2.2 Preparation of binary catalyst.....	30
3.2.2.3 Preparation of ternary catalyst.....	31
3.2.3 Preparation of ink.....	31



3.3 Characterization techniques.....	32
3.3.1 Cyclic voltammetry.....	32
3.3.2 Linear sweep voltammetry.....	35
3.3.3 Chronoamperometry.....	36
3.3.4 Electrochemical impedance spectrometry.....	37
3.3.5 Inductively coupled plasma – atomic emission spectrometry.....	38
3.3.6 Transmission electron microscopy.....	40
3.3.7 Energy dispersion spectroscopic analysis (EDS) in scanning electron microscope (SEM).....	41
3.3.8 X-ray diffraction.....	42
3.4 References .....	44
Chapter 4: results and discussion.....	46
4. Introduction.....	46
4.1 Physical properties.....	46
4.2 HR-TEM analysis.....	48
4.3 EDS analysis.....	50
4.4 X-ray diffraction analysis.....	53
4.5 Cyclic voltammetry study.....	55
4.6 Linear sweep voltammetry study.....	57
4.7 Electrochemical impedance spectrometry study.....	67
4.8 Chronoamperometry study.....	79
4.9 References.....	85
5. Chapter 5: Conclusion and recommendations.....	86
5.1 Conclusion.....	86
5.2 Recommendations.....	87



## List of figures

Figure 1.1	Schematic diagram of fuel cell.....7
Figure 3.1	Cyclic voltammogram of of Pd/MWCNT (at the fifth cycle) in 2 M KOH SOLUTION. Pd loading $17 \mu\text{g cm}^{-2}$ . Scan rate: $50 \text{ mV s}^{-1}$ .....33
Figure 4.1	Figure 4.1 HRTEM images of a)Pd ,b) PdNi,c) PdNiO,d) PdMn <sub>3</sub> O <sub>4</sub> and e)PdMn <sub>3</sub> O <sub>4</sub> NiO in-house electro-catalysts on MWCNT
Figure 4.2	EDX spectra of a) Pd, b) PdNi, c) PdNiO d) PdMn <sub>3</sub> O <sub>4</sub> , e) PdMn <sub>3</sub> O <sub>4</sub> NiO in-house electro-catalyst on MWCNT support.....79
Figure 4.3	x-ray diffraction of Pd, PdNi, PdMn, PdNiO, PdMn <sub>3</sub> O <sub>4</sub> and PdMn <sub>3</sub> O <sub>4</sub> NiO in-house electro-catalysts on MWCNT support.....83
Figure 4.4	Cyclic voltammetry of Pd, PdNi, PdMn, PdNiO, PdMn <sub>3</sub> O <sub>4</sub> and PdMn <sub>3</sub> O <sub>4</sub> NiO in-house electro-catalysts on MWCNT support in N <sub>2</sub> saturated 1.0M KOH at a scan rate of $30 \text{ mV} \cdot \text{s}^{-1}$ .....46
Figure 4.5	Linear sweep voltammetry of Pd in-house electro-catalysts on MWCNT support in N <sub>2</sub> saturated 1.0M KOH comparing the activity in 1M ethanol and 1M glycerol at a scan rate of $30 \text{ mV s}^{-1}$ .....48
Figure 4.6	Linear sweep voltammetry of PdNi in-house electro-catalysts on MWCNT support in N <sub>2</sub> saturated 1.0M KOH comparing the activity in 1M ethanol and 1M glycerol at a scan rate of $30 \text{ mV s}^{-1}$ .....49
Figure 4.7	Linear sweep voltammetry of PdNiO in-house electro-catalysts on MWCNT support in N <sub>2</sub> saturated 1.0M KOH comparing the activity in 1M ethanol and 1M glycerol at a scan rate of $30 \text{ mV s}^{-1}$ .....50

Figure 4.8	Linear sweep voltammetry of PdMn <sub>3</sub> O <sub>4</sub> in-house electro-catalysts on MWCNT support in N <sub>2</sub> saturated 1.0M KOH comparing the activity in 1M ethanol and 1M glycerol at a scan rate of 30mV s <sup>-1</sup> .....	51
Figure 4.9a)	Linear sweep voltammetry of PdMn <sub>3</sub> O <sub>4</sub> NiO in-house electro-catalysts on MWCNT support in N <sub>2</sub> saturated 1.0M KOH comparing the activity in 1M ethanol and 1M glycerol at a scan rate of 30mV s <sup>-1</sup> .....	52
Figure 4.9 b)	shows a zoomed in figure of Linear sweep voltammetry of PdMn <sub>3</sub> O <sub>4</sub> NiO in-house electro-catalysts on MWCNT support in N <sub>2</sub> saturated 1.0M KOH comparing the activity in 1M ethanol and 1M glycerol at a scan rate of 30mV s <sup>-1</sup> .....	52
Figure 4.10	Linear sweep voltammetry of Pd, PdNi, PdNiO, PdMn <sub>3</sub> O <sub>4</sub> and PdMn <sub>3</sub> O <sub>4</sub> NiO in-house electro-catalysts on MWCNT support in N <sub>2</sub> saturated 1.0M KOH with 1.0M ethanol at a scan rate of 30mV support in N <sub>2</sub> saturated 1.0M KOH comparing the activity in 1M ethanol and 1M glycerol at a scan rate of 30mV s <sup>-1</sup> .....	53
Figure 4.11	Linear sweep voltammetry of Pd, PdNi, PdMn, PdNiO, PdMn <sub>3</sub> O <sub>4</sub> and PdMn <sub>3</sub> O <sub>4</sub> NiO in-house electro-catalysts on MWCNT support in N <sub>2</sub> saturated 1.0M KOH with 1.0M glycerol at a scan rate of 30mV support in N <sub>2</sub> saturated 1.0M KOH comparing the activity in 1M ethanol and 1M glycerol at a scan rate of 30mVs <sup>-1</sup> .....	56

Figure 4.12	Impedance of Pd in-house electro-catalysts on MWCNT support in N <sub>2</sub> saturated 1.0M KOH comparing the activity in 1M ethanol at -0.1V and -0.3V.....	58
Figure 4.13	Impedance of Pd in-house electro-catalysts on MWCNT support in N <sub>2</sub> saturated 1.0M KOH comparing the activity in 1M glycerol at -0.1V and -0.3V.....	59
Figure 4.14	Impedance of PdNi in-house electro-catalysts on MWCNT support in N <sub>2</sub> saturated 1.0M KOH comparing the activity in 1M ethanol at -0.1V and -0.3V.....	60
Figure 4.15	Impedance of PdNi in-house electro-catalysts on MWCNT support in N <sub>2</sub> saturated 1.0M KOH comparing the activity in 1M glycerol at -0.1V and -0.3V.....	61
Figure 4.16	Impedance of PdNiO in-house electro-catalysts on MWCNT support in N <sub>2</sub> saturated 1.0M KOH comparing the activity in 1M ethanol at -0.1V and -0.3V.....	62
Figure 4.17	Impedance of PdNiO in-house electro-catalysts on MWCNT support in N <sub>2</sub> saturated 1.0M KOH comparing the activity in 1M glycerol at -0.1V and -0.3V.....	63
Figure 4.18	Impedance of PdMn <sub>3</sub> O <sub>4</sub> in-house electro-catalysts on MWCNT support in N <sub>2</sub> saturated 1.0M KOH comparing the activity in 1M ethanol at -0.1V and -0.3V.....	64

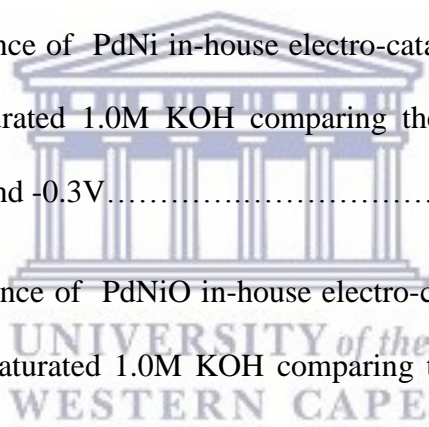


Figure 4.19	Impedance of PdMn3O4 in-house electro-catalysts on MWCNT support in N2 saturated 1.0M KOH comparing the activity in 1M glycerol at -0.1V and -0.3V.....	65
Figure 4.20	Impedance of PdMn3O4NiO in-house electro-catalysts on MWCNT support in N2 saturated 1.0M KOH comparing the activity in 1M ethanol at -0.1V and -0.3V.....	66
Figure 4.21	Impedance of PdMn3O4NiO in-house electro-catalysts on MWCNT support in N2 saturated 1.0M KOH comparing the activity in 1M glycerol at -0.1V and -0.3V.....	67
Figure 4.22	Impedance of Pd, PdNi, PdMn, PdNiO, PdMn3O4 and PdMn3O4NiO in-house electro-catalysts on MWCNT support in N2 saturated 1.0M KOH comparing the activity in 1M ethanol at -0.3V.....	68
Figure 4.23	Impedance of Pd, PdNi, PdMn, PdNiO, PdMn3O4 and PdMn3O4NiO in-house electro-catalysts on MWCNT support in N2 saturated 1.0M KOH comparing the activity in 1M glycerol at -0.3V.....	69
Figure 4.24	Chronoamperometry of Pd in-house electro-catalysts on MWCNT support in N2 saturated 1.0M KOH comparing the stability in 1M ethanol and 1M glycerol at a -0.2V.....	70
Figure 4.25	Chronoamperometry of PdNi in-house electro-catalysts on MWCNT support in N2 saturated 1.0M KOH comparing the stability in 1M ethanol and 1M glycerol at -0.2V.....	71

Figure 4.26	Chronoamperometry of PdNiO in-house electro-catalysts on MWCNT support in N <sub>2</sub> saturated 1.0M KOH comparing the stability in 1M ethanol and 1M glycerol at -0.2V.....	72
Figure 4.27	Chronoamperometry of PdMn <sub>3</sub> O <sub>4</sub> in-house electro-catalysts on MWCNT support in N <sub>2</sub> saturated 1.0M KOH comparing the stability in 1M ethanol and 1M glycerol at -0.2V.....	73
Figure 4.28	Chronoamperometry of PdMn <sub>3</sub> O <sub>4</sub> NiO in-house electro-catalysts on MWCNT support in N <sub>2</sub> saturated 1.0M KOH comparing the stability in 1M ethanol and 1M glycerol at -0.2V.....	74
Figure 4.29 a)	Chronoamperometry of Pd, PdNi, PdNiO, PdMn <sub>3</sub> O <sub>4</sub> and PdMn <sub>3</sub> O <sub>4</sub> NiO in-house electro-catalysts on MWCNT support in N <sub>2</sub> saturated 1.0M KOH with 1.0M ethanol at -0.2V.....	75
Figure 4.29 b)	Zoomed in view of Chronoamperometry of Pd, PdNi, PdNiO, PdMn <sub>3</sub> O <sub>4</sub> and PdMn <sub>3</sub> O <sub>4</sub> NiO in-house electro-catalysts on MWCNT support in N <sub>2</sub> saturated 1.0M KOH with 1.0M ethanol at -0.2V.....	75
figure 4.30a)	Chronoamperometry of Pd, PdNi, PdNiO, PdMn <sub>3</sub> O <sub>4</sub> and PdMn <sub>3</sub> O <sub>4</sub> NiO in-house electro-catalysts on MWCNT support in N <sub>2</sub> saturated 1.0M KOH with 1.0M ethanol at -0.2V.....	76
Figure 4.30 b)	Zoomed in view of Chronoamperometry of Pd, PdNi, PdNiO, PdMn <sub>3</sub> O <sub>4</sub> and PdMn <sub>3</sub> O <sub>4</sub> NiO in-house electro-catalysts on MWCNT support in N <sub>2</sub> saturated 1.0M KOH with 1.0M ethanol at -0.2V.....	76

## **List of tables**

Table 3.1	List of chemicals used for the study, and their suppliers.....	28
Table 3.2	Sample preparation and operating parameters for CV.....	34
Table 3.3	Sample preparation and operating parameters for LSV.....	35
Table 3.4	Sample preparation and operating parameters for chronoamperometry.....	36
Table 3.5	Sample preparation and operating parameters for electrochemical impedance spectrometry.....	37
Table 3.6	ICP operating conditions for determination of Pd, Ni and Mn.....	39
Table 3.7	operating conditions for HR-TEM.....	41
Table 3.8	operating conditions for X-ray diffractometer.....	43
Table 4.1	Values of particle size and metal loading for the in-house catalysts...46	
Table 4.2	ECSA values of 20% Pd, PdNi, PdNiO, PdMn <sub>3</sub> O <sub>4</sub> and PdMn <sub>3</sub> O <sub>4</sub> NiO in-house electro-catalysts on MWCNT.....	56
Table 4.3	Current density values and onset potentials of 20% Pd, PdNi, PdNiO, PdMn <sub>3</sub> O <sub>4</sub> and PdMn <sub>3</sub> O <sub>4</sub> NiO in-house electro-catalysts on MWCNT 1.0M KOH with 1.0M ethanol at a scan rate of 30mV.....	64
Table 4.4	Current density values and onset potentials of 20% Pd, PdNi, PdNiO, PdMn <sub>3</sub> O <sub>4</sub> and PdMn <sub>3</sub> O <sub>4</sub> NiO in-house electro-catalysts on MWCNT 1.0M KOH with 1.0M glycerol at a scan rate of 30mV.....	66

## **List of abbreviations**

PEMFC	Proton exchange membrane fuel cell
SOFC	Solid oxide fuel cell
PAFC	Phosphoric acid fuel cell
MCFC	Molten carbonate fuel cell
AFC	Alkaline fuel cell
AOR	Alcohol oxidation reaction
MWCNT	Multi walled carbon nanotube
DAFC	Direct alcohol fuel cell
DMFC	Direct methanol fuel cell
Pt	Platinum
Pd	Palladium
DEFC	Direct ethanol fuel cell
DGFC	Direct glycerol fuel cell
CV	cyclic voltammetry
LSV	linear sweep voltammetry
EIS	electrochemical impedance spectrometry

HR-TEM	high resolution transmission electron microscopy
EDS	electron dispersive spectrometry
XRD	x-ray diffraction
ICP	inductive coupled plasma
ECSA	electrochemical surface area



UNIVERSITY *of the*  
WESTERN CAPE

## CHAPTER 1

### 1 Chapter overview

This chapter looks at the energy demand worldwide with the aim of pointing out the importance of renewable energy sources as an alternative to fossil fuels. There are many different types of available renewable energy sources, and this chapter focuses on fuel cells, the need for developing affordable catalysts material for the fuel cell system. The aim and objectives of the research project and thesis outline are highlighted towards the end of the chapter.

#### 1.1 Background

The world population is ever increasing and technology always being improved upon, this has led to the increase in the demand of fossil fuels. This demand can no longer be met by our remaining fossil fuel reserves, and so this means alternative ways of energy have to be found. A recent study conducted by the World Energy Council showed that the energy demand will have increased by 50-80% from 1990 to 2020. This increasing demand will have a significant strain on the current energy infrastructure and will potentially damage the world environment health by CO, CO<sub>2</sub>, SO<sub>2</sub>, NO<sub>x</sub>, and waste gas emissions and global warming [1]. It has been reported that the need for oil globally has risen to a thousand barrels a second and that is approximately two litres of oil per person in the world, this global consumption is equivalent to thirteen terawatts of power demand [2]. In developing countries it has been reported that an average person consumes an equivalent of 6 barrels per annum, whereas in developed countries on average a person consumes 40 barrels of oil per annum [3].

Oil is not the only non-renewable energy source that is depleting. There are two other types of non-renewable energy sources namely; coal and natural gas. It is approximated that the three non-renewable energy resources will deplete by 2112, with only coal reserves being

available in 2042 [4]. Coal is the most abundant of the fossil fuels; however coal generates the most airborne pollutants. This has led to coal fired electricity generating plants being slowly replaced by gas fired plants. The most energy efficient and cleanest burning fossil fuel is natural gas, but its supply is hindered by insufficient extraction and transportation infrastructure. Example regasification and storage facilities for liquefied natural gas are a challenge. Petroleum derivatives offer versatility in use and ease of transport that make them ideal for transportation sector, it is therefore important to note that none of the three major fossil fuels is a perfect substitute for each other [5].

The non-renewable energy resources are of great value for the current generation as they are for future generations. It is important to make sure that they do not deplete. Pretty soon all of man's energy needs will need to be provided using sources of energy that is clean and not dependent on fossil fuels.

The climate warming has been blamed on industrial companies for their use of fossil fuels. When burning fossil fuels like coal, oil and natural gas, harmful gases are released into the atmosphere which will in turn trap heat in the atmosphere and cause global warming. There has been an on-going debate between scientists to distinguish between the changes that are human induced and those due to natural climate variability. The highest emission levels are from industrialized countries and they must take the most responsibility for global warming. Developing countries must also take action to avoid future increases in emission levels as their economies develop and population grows [5]. CO<sub>2</sub> (carbon dioxide) emission is greatly produced from human activities. Fossil fuel production is the most significant contributor to potential climate change and primarily CO<sub>2</sub> emission [5, 6].

Renewable energy is the solution to the growing energy challenges and CO<sub>2</sub> emission. Renewable energy resources such as solar, wind, biomass, and wave and tidal energy, are abundant, inexhaustible and environmentally friendly.

The efficiency of most energy technologies has been characterized. The ones having the highest efficiency are the large electrical generators 98-99% efficient and motors 90-97% efficient. Rotating heat engines that are limited by the second law of thermodynamics follow with the second highest efficiency: gas and steam turbines 30-50%, diesel 30-50% and internal combustion 15-25% engines. Electrolyte, electrode materials and catalysts currently limit fuel cells with an efficiency of 50-55%; with the hopes of it eventually being 70%. Heat engines will be likely replaced by fuel cells that run with hydrogen [6]. Fuel cells however unlike the former energy technologies, still face challenges to compete in the commercial market. Renewable energy converters which include PV (photovoltaic) cells; commercial arrays are at about 15-20% the theoretical peak for single band gap crystalline cells. It is approximated at 24% for multiband cells and the efficiency drops even lower for more cost effective amorphous thin films. With wind turbines, commercial units are around 30-40% and theoretically “Betz limit” approximated at 59%. High-pressure sodium vapour is at an efficiency of 15-20%, fluorescent 10-12% and incandescent 2-5% efficiency with illumination generating more heat than light. Photosynthesis has a very low sunlight-to-chemical energy efficiency, limited by chlorophyll absorption bands, most productive ecosystems are about 1 to 2% efficient; theoretical peak independent of cell or ecosystem is approximately 8% [7].

Renewable energy sources have a lower efficiency compared to fossil fuels, making it difficult to have renewable energy sources as fossil fuel replacements. However fuel cells have a high efficiency compared to photovoltaic cells and wind turbines, and emit no

greenhouse gases so this makes fuel cells a good candidate to replace or work with fossil fuels to decrease greenhouse gases [7].

Scientists and engineers are now challenged to see if they can help in solving the energy problem that is currently faced. Some serious questions have to be answered by the world population, such as how long can the earth's resources continue to be exploited and live these high energy demanding lifestyles before the tipping point is reached, where there is no turning back from the chaos caused.

This has caused researchers to look into fuel cells as one of the renewable energy sources to deal with the energy crisis. Their reliability is still evolving; also there are safety concerns with hydrogen fuel cells and also with hydrogen not being readily available. The fuel used for fuel cells also has a low density compared to gasoline. Although fuel cells have their fair share of drawbacks they hold promise for our energy crisis in the future. Fuel cells have a high efficiency, and they use renewable fuels. Fuel cells can run continuously as long as fuel is available, they do not require recharging. Another advantage of fuel cells is that they can run in reverse for energy storage, producing hydrogen from electricity and water.

Fuel cells are environmentally friendly energy sources for the twenty first century that could be our solution to the energy and global warming crisis. They are thought to be one of the solutions because they can directly convert chemical energy to electrical energy without emitting any greenhouse gases. Per the Department of Energy of the United States, Christian Friedrich Schönbein discovered the fuel cell concept. His work was then published a Philosophical magazine in 1839. Per Grimes, Sir William Grove who also published his work in Philosophical magazine in 1839 but in February devised the fuel cell.

Fuel cells are then seen as the emerging alternative technology to the more polluting internal combustion engines in vehicle and stationary distributed energy applications. The future

demand for portable electric power supplies is most likely to exceed the capability of current battery technology [8]. Fuel cells offer a very attractive technology evolution path in that they can deliver significant efficiency gains on today's commercially available hydrocarbon fuels while also offering high efficiency in the future when hydrogen becomes widely available. The key and technical challenges facing fuel cells are cost reduction and increased durability of materials and components [9].

Unlike a battery a fuel cell is a device that continuously generates electricity at low temperatures, electrochemical reactions of hydrogen and oxygen from air. The major difference between a battery and a fuel cell is that batteries store electricity while fuel cells operate continuously producing electricity as long as fuel and air are supplied. Any hydrogen rich fuel can be used in different types of fuel cells, but using a hydrocarbon-based fuel inevitably leads to CO<sub>2</sub> emission. Hydrogen powered fuel cells emit only water and have virtually no pollutant emissions, even nitrogen oxides because they operate at temperatures that are much lower than the internal combustion engine. However fuel cells, fuelled with hydrocarbon fuels have the potential to provide efficient, clean and quiet energy conversion, which can contribute to a significant reduction in greenhouse gases and local pollution. In transportation hydrogen fuel cell engines operate at an efficiency of up to 65%, compared to the 25% for present-day petrol-driven car engines. When heat generated in fuel cells is also utilised in combined heat and power (CHP) system an overall efficiency in excess of 85% can be achieved [8].

Fuel cells are widely efficient power sources, offering high energy densities and energy efficiency compared to other conventional systems.

## 1.2 Overview of fuel cells

A fuel cell is a device that converts the chemical energy of a fuel (e.g. hydrogen, ethanol, glycerol etc.) and oxidant in the presence of a catalyst into electricity, heat and water. Fuel cells may lead to an innovative enhancement in energy production and before long they could become the next true world economy, having an impact related to the current petroleum and oil markets. Fuel cells are economically feasible for commercial energy production and the developed fuels are being more competent for energy production [9, 10, 11].

Nowadays the types of fuel cells are differentiated by their electrolytes; Proton exchange membrane fuel cell (PEMFCs), solid oxide fuel cell (SOFCs), phosphoric acid fuel cell (PAFCs), molten carbonate fuel cell (MCFCs) and Alkaline fuel cell (AFCs).

Fuel cells can vary from tiny devices that produce a few watts of electricity to large power plants producing megawatts of electricity. Fuel cells are based around a central design using two electrodes separated by a solid or liquid electrolyte that carries electrically charged particles between them. A catalyst is usually used to speed up the reactions at the electrodes.

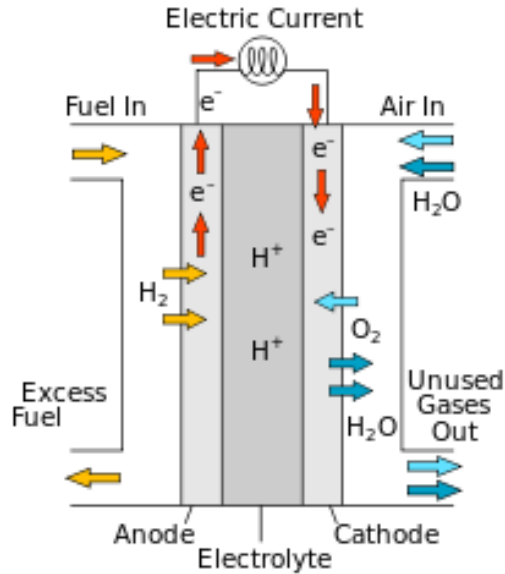


Figure 1.1: Schematic diagram of a fuel cell. [12]

The first type of fuel cell to be put into practical use was the;

1) Alkaline fuel cell at the start of the twentieth century [8]. They used potassium hydroxide (KOH) as the electrolyte. The alkaline fuel cell made it possible to generate electricity from hydrogen. The National Aeronautics and Space Administration (NASA) in the 1950s used AFC system and technology and they still use this technology for today's space shuttle missions. By the 1970s a car had been built by Kordesch which ran on alkaline fuel cells and lead-acid battery, because many research groups started to focus on the AFC for applications. Even though there was this early success with the AFC interest in its technology then started to drop due to economic factors, material problems and certain inadequacies in the operation of electrochemical devices. Development and advances in the other form of fuel cells in the past two decades has again sparked interest in the AFCs.

Other types of fuel cells include:

2) Proton Exchange Membrane Fuel Cells (PEMFC), these are water-based, polymer electrolyte membrane fuel cells. They use platinum based catalyst on both electrodes and are generally hydrogen fuelled. PEMFC generally operate at low temperatures, below 100°C and are ideal for vehicles [12, 13].

3) Phosphoric Acid Fuel Cells (PAFC), they use finely dispersed platinum catalyst on carbon and operate around 180°C. They have a relatively low efficiency but it can be raised to over 80% if the heat is used and PAFC are typically used in stationary power generators. The electrolyte of the PAFC is liquid phosphoric acid in a bonded silicon carbide matrix [14].

4) Solid Oxide Fuel Cell (SOFC), have a solid ceramic, such as stabilized zirconium oxide as the electrolyte. SOFC do not need a precious metal as a catalyst, they can run on hydrocarbons such as methane. They operate at very high temperatures of 800°C-1000°C and are mostly employed in stationary power generation [15, 16].

5) Molten Carbonate Fuel Cells (MCFC) like the SOFC the MCFC do not need a special catalyst and can run on hydrocarbon fuels like methane. They operate at 650°C and best run continuously due to high operating temperatures. Most fuel cell power plants of megawatt capacity use the MCFCs and so do large combined heat and power plants. The electrolyte of a MCFC is a molten carbonate salt suspended in a porous ceramic matrix [17, 18].

6) Direct Methanol Fuel Cells (DMFC), use a polymer membrane as an electrolyte and use a platinum-ruthenium catalyst on the anode and a platinum catalyst on the cathode. The DMFC operate in the range of 60°C-130°C and are convenient for portable power applications with

outputs generally less than 250 Watts. The DMFC can draw hydrogen atoms from liquid methanol, which is used as fuel instead of pure hydrogen giving the cell its name [20, 21].

Recently other types of alcohols have been researched for these types of fuel cells hence they are also known as Direct Alcohol Fuel Cells (DAFC). This type of fuel cell uses other hydrocarbons e.g. ethanol and glycerol other than methanol. These fuels have been looked at for the DAFC. Ethanol and glycerol which are used in this study are non-toxic fuels and are easily produced, unlike methanol which is toxic to humans [22].

### **1.3 Rational of research project**

One of the major problems associated with the DAFC deals with the anode side of the fuel cell where oxidation of the fuel produces  $\text{CO}_2$ . The corrosion of the anode catalyst with time results in a considerable loss in the overall efficiency of the DAFC and the high cost of the platinum catalyst.

This has led to intensive research being undertaken in order to address the problems associated with the DAFC which can be traced back to the catalyst used at the electrode surfaces. A considerable amount of time and effort has been expended in addressing this problem and finding lasting solutions. The cost related to platinum as a catalyst has led to other metals being researched as a fuel cell catalyst and palladium due to its chemical properties and more abundant than platinum has drawn interest from researchers. In light of this fact the development of research goals with regard to the project were developed.

### **1.4 Aims and objectives:**

The aim of the project is to develop catalysts for DAFC for the alcohol oxidation reaction (AOR). The objectives are as follows; to synthesize catalyst on multiwall carbon nanotube support material. The catalysts properties were evaluated in a half cell using analytical

electrochemical techniques such Cyclic Voltammetry, Linear Sweep Voltammetry, Chronoamperometry and Electrochemical Impedance spectroscopy. The physical characterization of the synthesized catalysts was done using analytical techniques such as High Resolution Transmission Electron Microscopy, Induced Coupled Plasma and X-ray Diffraction Spectroscopy.

- To promote the improvement in the activity and efficiency of the proposed catalysts.

## **1.5 Thesis outline**

### **Chapter 2: literature review**

Important concepts relating electro-catalysis to fuel cell are presented in this chapter. The various carbon support materials for fuel cell electrodes are briefly looked into with informed choice into the choice of support for this proposed work. The different synthetic routes for synthesizing catalysts are also presented in this chapter with the focus on the synthesis method used in this work. The chapter aims at providing a concise and informative guide to the literature consulted for the proposed thesis.

### **Chapter 3: Materials and methods**

In this chapter a description of the materials and methods used in the proposed work is given. The materials and synthetic route is explained in detail. The different physicochemical and electrochemical techniques used to characterize the different catalysts are briefly explained in the chapter.

### **Chapter 4: Results and discussion**

This chapter focuses on the obtained results for physicochemical and electrochemical characterization of the catalysts synthesized using sodium borohydride as a stabilizer in the polyol method.

### **Chapter 5: Conclusions and recommendation**

This chapter gives the overall conclusion of the work completed in the thesis and future recommendations for fuel cell catalyst synthesis and characterization.



## References

1. Omer, A.M., **2008**. Energy, environment and sustainable development. *Renewable and sustainable energy reviews*, 12(9), pp.2265-2300.
2. BP Global, BP Statistica Review of world Energy June **2016**. Viewed 28 January **2017**[https://www.google.co.za/?gfe\\_rd=cr&ei=FjaYWI7CJI2p8weVrY\\_ADw#q=bp+world+review+of+world+energy+2016](https://www.google.co.za/?gfe_rd=cr&ei=FjaYWI7CJI2p8weVrY_ADw#q=bp+world+review+of+world+energy+2016).
3. Chow, J., Kopp, R.J. and Portney, P.R., **2003**. Energy resources and global development. *Science*, 302(5650), pp.1528-1531.
4. Shafiee, S. and Topal, E., **2009**. When will fossil fuel reserves be diminished?. *Energy policy*, 37(1), pp.181-189.
5. Kennedy, D. ed., **2006**. *Science Magazine's State of the Planet 2006-2007*. Island Press.
6. Nordhaus, W.D., **1991**. To slow or not to slow: the economics of the greenhouse effect. *The economic journal*, 101(407), pp.920-937
7. Hoffert, M.I., Caldeira, K., Benford, G., Criswell, D.R., Green, C., Herzog, H., Jain, A.K., Khesghi, H.S., Lackner, K.S., Lewis, J.S. and Lightfoot, H.D., **2002**. Advanced technology paths to global climate stability: energy for a greenhouse planet. *science*, 298(5595), pp.981-987.
8. Edwards, P.P., Kuznetsov, V.L., David, W.I. and Brandon, N.P., **2008**. Hydrogen and fuel cells: towards a sustainable energy future. *Energy policy*, 36(12), pp.4356-4362.
9. Carrette, L., Friedrich, K.A. and Stimming, U., 2001. Fuel cells—fundamentals and applications. *Fuel cells*, 1(1), pp.5-39.
10. Dutta, S., **2014**. A review on production, storage of hydrogen and its utilization as an energy resource. *Journal of Industrial and Engineering Chemistry*, 20(4), pp.1148-1156.

11. Badwal, S.P.S., Giddey, S., Kulkarni, A., Goel, J. and Basu, S., **2015**.  
Direct ethanol fuel cells for transport and stationary applications—A  
comprehensive review. *Applied Energy*, 145, pp.80-103..
12. [https://en.wikipedia.org/wiki/Proton\\_exchange\\_membrane\\_fuel\\_cell](https://en.wikipedia.org/wiki/Proton_exchange_membrane_fuel_cell)
13. Ralph, T.R., **1997**. Proton exchange membrane fuel cells. *Platinum  
metals review*, 41(3), pp.102-113.
14. [https://en.wikipedia.org/wiki/Phosphoric-acid\\_fuel\\_cell](https://en.wikipedia.org/wiki/Phosphoric-acid_fuel_cell)
15. [https://en.wikipedia.org/wiki/Solid\\_oxide\\_fuel\\_cell](https://en.wikipedia.org/wiki/Solid_oxide_fuel_cell)
16. Ishihara, T. and Misawa, H., Ngk Insulators, Ltd., **1993**. *Solid oxide fuel cells*. U.S.  
Patent 5,185,219.
17. [https://en.wikipedia.org/wiki/Molten\\_carbonate\\_fuel\\_cell](https://en.wikipedia.org/wiki/Molten_carbonate_fuel_cell)
18. Hatoh, K., Niikura, J., Yasumoto, E. and Gamou, T., Matsushita Electric Industrial  
Co., Ltd., **1996**. *Molten carbonate fuel cell*. U.S. Patent 5,589,287.
19. [https://en.wikipedia.org/wiki/Alkaline\\_fuel\\_cell](https://en.wikipedia.org/wiki/Alkaline_fuel_cell)
20. [https://en.wikipedia.org/wiki/Direct-ethanol\\_fuel\\_cell](https://en.wikipedia.org/wiki/Direct-ethanol_fuel_cell)
21. Vigier, F., Rousseau, S., Coutanceau, C., Leger, J.M. and Lamy, C., **2006**.  
Electrocatalysis for the direct alcohol fuel cell. *Topics in Catalysis*, 40(1), pp.111-121.
22. Bambagioni, V., Bianchini, C., Marchionni, A., Filippi, J., Vizza, F., Teddy, J., Serp,  
P. and Zhiani, M., **2009**. Pd and Pt–Ru anode electrocatalysts supported on multi-  
walled carbon nanotubes and their use in passive and active direct alcohol fuel cells  
with an anion-exchange membrane (alcohol= methanol, ethanol, glycerol). *Journal of  
Power Sources*, 190(2), pp.241-251.

## **CHAPTER 2: Literature review**

### **2. Chapter overview**

This chapter covers the literature review on fuel cell. It looks at the components of the anode catalyst and also looks into the literature for the different alcohols used in fuel cells. Literature on the different synthesis methods for fuel cell catalysts is reviewed and also the chapter looks at the support materials for fuel cell catalysts.

#### **2.1 Direct alcohol fuel cells**

Direct alcohol fuel cells are getting more attention as an alternative energy source, due to their storage being much easier compared to hydrogen. Direct alcohol fuel cells (DAFC) have attracted an increasing interest as a power source for portable application [1]. The alcohols such as ethanol, methanol, glycerol, and ethylene glycol exhibit high volumetric density [2].

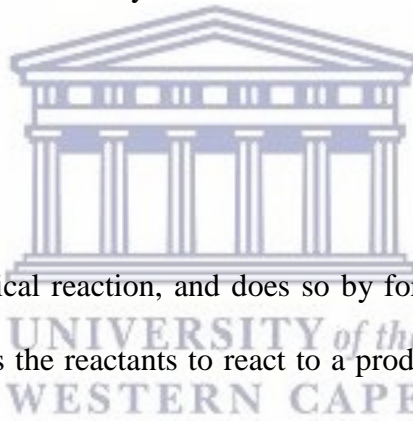
The most common DAFC is the direct methanol fuel cell, of which there exist commercial devices with power starting from a few watts to 100 W [3]. Large majorities of DMFCs operate in acidic media with the anode catalyst containing Pt and make use of solid electrolyte constituted by proton exchange membrane of the Nafion family. DAFCs however suffer some disadvantages like; CO poisoning of the Pt-based catalyst, effective alcohol crossover, degradation of the membrane, and corrosion of the carbon materials and cell hardware [4]. This results in fuel utilization and cell voltage being lower than expected.

In the last few years efforts have been put into looking at other fuels as an alternative. Using ethanol as an alternative fuel for DAFC has some benefits. Research has shown that ethanol can permeate through the electrolyte like it does for methanol in DMFC resulting in methanol crossover, but with less of an effect on the fuel cell performance. Although the crossover is not as affective to the cell performance, it is not negligible [5]. Unlike methanol which is

toxic to human beings, ethanol is a non-toxic fuel and is naturally available, because it can be massively produced from biomass feed stocks originating from agriculture (first generation bioethanol), and forestry and urban residues (second generation bioethanol) [3, 6, 7]. Another great advantage to using ethanol is the renewability, high power density and zero greenhouse contribution to the environment [6].

Glycerol is also a low toxicity fuel and easily available. The fuel is a by-product of biodiesel production and because of this it is inexpensive [7]. Glycerol is a polyol alcohol that displays energy densities that are relatively comparable to that of gasoline. The energy densities for alcohols vary from 6.0 kWh kg<sup>-1</sup> for methanol to 10 kWh kg<sup>-1</sup> for heavy alcohols [8]. Both of the fuels discussed were used in this study.

## 2.2 Catalysts



A catalyst accelerates a chemical reaction, and does so by forming bonds with the reacting molecules. The catalyst allows the reactants to react to a product, which then detaches from the catalyst and leaves it unaltered such that it is available for the next reaction. A catalytic reaction can thus be described as a cyclic event in which the catalyst precipitates and is recovered in its original state at the end of the cycle.

In industry catalysts are the workhorses of chemical transformations and approximately 85-90% of chemical products in industry are made with catalytic processes. A catalyst offers an alternative, energetically favourable mechanism to the non-catalytic reaction, thus enabling processes to be carried out under industrially feasible conditions of pressure and temperature.

### **2.2.1 Catalysts used in fuel cells**

Different catalysts are used in fuel cells. The use for different catalyst is caused by the need to improve the performance of the fuel cell, namely the durability, stability and activity of the fuel cell and also to reduce cost. The catalysts a fuel cell uses are classified as heterogeneous, and this is due to the fact that the catalysts used for fuel cells are normally noble metals immobilized on a conductive support. A heterogeneous catalyst functions in a different phase to the reactants. An example of this heterogeneous catalyst is a nickel catalyst in the hydrogenation of vegetable oil. In this reaction, the vegetable oil is in liquid state and the Ni catalysts in solid phase. Heterogeneous catalyst is usually supported and this means the catalyst is dispersed on a secondary material to increase its surface area and this enhances the effect [9, 10].

Fuel cell catalysts are classified according to specific reactions they would undergo. In the DAFC the catalysts would either be referred to as an anode catalyst or a cathode catalyst. The anode is where alcohol oxidation takes place and the anode catalyst would need to be able to perform this function. The cathode catalyst would usually be used in reducing reactants at the cathode end of the fuel cell and it also needs to meet certain requirements [11, 12]. The different most commonly used catalysts in fuel cells are Pd and Pt, and they are usually alloyed with metals like ruthenium, nickel, manganese, gold and tin. In this work Pd catalysts was used for alcohol oxidation reaction.

### **2.2.2 Palladium a catalyst for fuel cells**

The cost and scarcity of the Pt-based catalyst has led to finding catalysts that are able to perform at reasonable efficiency but cutting the cost of the fuel cell. Palladium has shown promise in oxidizing several alcohols, including ethanol and glycerol in alkaline media [7] and it is much cheaper and more abundant compared to platinum. new research is now

looking at designing catalytic structures for DAFC anodes that do not contain platinum, or only small trace amounts of this rare metal, because this will result in the cost for production being cheaper [7-9]. It is important that the palladium even though it is cheaper, but it can oxidize primary and secondary alcohols with fast kinetics and tolerable deactivation. Pd based electro-catalyst can be highly active for the oxidation of a large variety of substrates in alkaline environments, where also non-noble metals are sufficiently stable for electrochemical applications [7]. Research from Shen and co-workers had Pd binary catalysts exhibiting higher catalytic activity and stability compared to Pt in alkaline media [14]. Pd has a higher activity for ethanol oxidation reaction (EOR) compared to Pt and this is accredited to its more oxophilic nature that enables oxidative desorption of intermediate species[4]. The same rationale is behind introducing Ni in electro-catalyst for the EOR [13].

### **2.2.3 Palladium binary catalysts as anode catalyst for fuel cells**

. Palladium and palladium alloys not only showed they are able to oxidize the non-toxic alcohols but some studies also showed the improvement in activity and stability for the Pd alloys [15,16]. The higher molecular weight alcohols have shown difficulty in being oxidized by platinum or platinum alloys supported on carbon blacks, no known anode catalysts based on platinum has demonstrated the capacity to produce acceptable power densities in either direct ethanol fuel cells (DEFC) or direct glycerol fuel cells (DGFC) even at high metal loading [17]. The difficulty encountered by the platinum and platinum alloy is not experienced by palladium binary catalysts, as they show great activity for DEFC and DGFC [16]. In this study Pd and Pd based catalysts were used as anodes for direct alcohol oxidation reactions.

## 2.3 Preparation methods for fuel cell catalysts

The method employed for the catalyst preparation has a great effect on the catalyst activity. There are different types of catalyst preparation. The methods that are used for catalyst preparation for fuel cells applications include the sulphite complex route, precipitation method, Bönemann method, and the polyol method just to name a few.

### 2.3.1 Sulphite complex route

This method involves the synthesis of Pt sulphite complexes in aqueous solution. The general starting metal precursor salts are  $\text{H}_2\text{PtCl}_6$  which is suspended in an aqueous solution containing  $\text{NaHSO}_3$ . This will then be subjected to oxidative decomposition with hydrogen peroxide. These particles are then adsorbed onto the carbon support material. The catalysts are then filtered and further subjected to heat treatment and reduced under flow of hydrogen gas. [18-20]. One of the main drawbacks in the preparation method is the presence of the chlorine contaminants in the as residues of chloride-based precursors [21].

### 2.3.2 Impregnation method

The impregnation method is seen as one of the most common and simplest methods for preparation of fuel cell catalysts. The method generally involves the impregnation of a metal salt solution onto a support after certain time intervals. The slurry is then heated to remove the solvent and the residue is subsequently reduced at elevated temperatures to decompose the salt and give rise to the desired catalyst. A variation of this method is known as the incipient wet impregnation method. A general reaction involves soaking a metal precursor ( $\text{PtCl}_6^{2-}$ ) into the pores of a support before the reduction step. The reduction step is usually carried out using borohydrides, hydrazines, formic acid or hydrogen gas depending on the desired results [22, 23]. A major challenge for this method is the use of the chloride

precursors that could lead to chloride poisoning which would result in lower catalytic activity and stability of the chloride-salt derived catalyst.

### **2.3.3 Bönneiman method**

Stabilized colloidal precursors are prepared via the reduction of anhydrous  $\text{PtCl}_2$ ,  $\text{RuCl}_3$  and  $\text{MoCl}_5$  dissolved in THF (tetrahydrofuran). A carbon support suspension in water purified in a Millipore is then impregnated with the appropriate amount of the colloidal solution. Thermal treatments are carried out in a  $\text{H}_2$  reducing atmosphere at  $300\text{ }^\circ\text{C}$  for 2 hours [24]. The disadvantages is that it involves a number of complicated and expensive steps and takes a fair amount of time.

### **2.3.4 Microemulsion method**

The microemulsion method may be defined as a method of dispersing immiscible liquid such that one of the liquids forms nanosized droplets by shaking, stirring or homogenising the mixture. As the definition states, the method generally involves the use of two immiscible liquids, example water and cyclohexane followed by the addition of a surfactant and reducing agent depending on desired result. To the homogenised mixture an appropriate amount of carbon support is added under constant stirring, washed with water and ethanol and dried under vacuum at room temperature [25, 26]. The disadvantage of the microemulsion method is the many washing steps and the requirements of expensive surfactants, which in return make scaling up not economical.

### **2.3.5 Vapour phase method**

In the vapour phase method used for the synthesis of nanoparticles, conditions are created where the vapour phase mixture is thermodynamically unstable relative to the formation of the solid material to be prepared in the nanoparticle form. There are two kinds of gas phase

reactions that are employed for the synthesis of nanoparticles. It is the two-step process which consists of the gas phase adsorption of the precursor on the support material, followed by the thermal treatments required to obtain the active catalyst and the other being a one-step process in which the precursor is simultaneously adsorbed and decomposed on the heated support [27].

### **2.3.6 Polyol method**

The polyol method is classified under the colloidal methods in the synthesis of catalysts. The approach is known as a bottom-up approach. The polyol method is a typical technique to prepare bimetallic metallic nanoparticles in solution by reducing their ionic salts [28]. In the polyol method a powdered inorganic metallic compound is suspended in a liquid polyol (ethyleneglycol). The suspension is stirred and heated to a given temperature. A complete reduction of the compounds can be achieved within a few hours and the recovered metal is a fine powder [29]. The method can also be carried out at room temperature and because no additional heat is required it means the reaction is less energy demanding and this is an advantage to upscale the reaction. When the reaction is carried out at room temperature, it generally employs sodium borohydride as a reducing agent [30].

The polyol method has been modified in some cases to obtain even smaller particles and a better dispersion. A drawback to the polyol method is choosing the suitable hydroxyl for individual processes.

A huge advantage for the polyol method however are the low operating temperatures, where the process can be able to control properties of the particles such as size, shape and uniformity. Unlike other methods such as the impregnation method and the sulphite complex route which have the presence of chlorine contaminants, the polyol method yields high pure organic free powders.

## **2.4 Supports for catalyst**

The stability of a supported catalyst is much higher than that of an unsupported catalyst, in terms of catalytic sites to the accumulation under fuel cell operating conditions. Carbon supports are mostly used supports for fuel cells. A good electronic conductivity of carbon support provides electron transfer from the catalytic sites to the conductive carbon electrodes and then to the external circuit.

### **2.4.1 Carbon black**

When any carbon containing material is heated in an inert, oxygen-free environment, it produces a material known as carbon black. Carbon black was once regarded as an amorphous form of carbon that contained almost spherical particles of graphite [32]. The particles are usually below 50nm in diameter that may cleave to form particle aggregates and agglomerates of around 250nm in diameter. The particles have para-crystallite structures where an assembly of parallel layers form non discrete 3D groupings [32]. The morphology and particle size distribution of carbon black is dependent on the source material and the process of its thermal decomposition. Particle size and distribution also determine the safe area and they are the most important properties of carbon black for end-use applications [32, 33].

### **2.4.2 Multi walled carbon nanotubes**

Layers of graphite rolled into cylindrical form and are often closed on both ends are known as carbon nanotubes. They can be synthesised in a laboratory and show impressive mechanical and thermal conductivity. Carbon nanotubes have also been proved to exhibit great electrical properties [32, 33]. Nanotubes exist with diameters of a few nanometers and lengths of the

order of 1mm, and they are able to entrap atoms of other elements in their molecular structure [32, 33].

The research uses multi walled carbon nanotubes (MWCNTs) as a catalyst support material because it is evident from previous studies that for low temperature fuel cells e.g. PEMFC and DMFC that have Pt supported on multi-walled carbon nanotubes exhibits better performance for electro-oxidation of alcohol than that on carbon black [34, 35]. Nano-structured carbon materials have been used due to their improved physical chemical properties. In this work CNT was chosen due to improved properties. Either than just good catalytic activity, a good support should possess good corrosion resistance; it has been proposed that carbon material with more graphite component can be more stable. Carbon nanotubes have been recently proposed as promising support material for fuel cell catalyst due to their unique characteristics, which include high aspect ratio, high electron conductivity, and high mass transport capability [35]. Active metal particles may disperse on the external walls or be encapsulated in the interior of the nanotubes due to the size and morphology of the CNTs. The metal particles on the external walls and the reactant molecules make contact more easily compared to those encapsulated in the internal channels of the CNTs [35].

## 2.5 References

1. Vishnyakov, V.M., **2006**. Proton exchange membrane fuel cells. *Vacuum*, 80(10), pp.1053-1065.
2. Fashedemi, O.O. and Ozoemena, K.I., **2014**. Comparative electrocatalytic oxidation of ethanol, ethylene glycol and glycerol in alkaline medium at Pd-decorated FeCo@Fe/C core-shell nanocatalysts. *Electrochimica Acta*, 128, pp.279-286.
3. Bianchini, C. and Shen, P.K., **2009**. Palladium-based electrocatalysts for alcohol oxidation in half cells and in direct alcohol fuel cells. *Chemical Reviews*, 109(9), pp.4183-4206
4. Cheng, X., Shi, Z., Glass, N., Zhang, L., Zhang, J., Song, D., Liu, Z.S., Wang, H. and Shen, J., **2007**. A review of PEM hydrogen fuel cell contamination: Impacts, mechanisms, and mitigation. *Journal of Power Sources*, 165(2), pp.739-756.
5. Lamy, C., Lima, A., LeRhun, V., Delime, F., Coutanceau, C. and Léger, J.M., **2002**. Recent advances in the development of direct alcohol fuel cells (DAFC). *Journal of Power Sources*, 105(2), pp.283-296.
6. Song, S. and Tsiakaras, P., **2006**. Recent progress in direct ethanol proton exchange membrane fuel cells (DE-PEMFCs). *Applied Catalysis B: Environmental*, 63(3), pp.187-193.
7. Bambagioni, V., Bianchini, C., Marchionni, A., Filippi, J., Vizza, F., Teddy, J., Serp, P. and Zhiani, M., **2009**. Pd and Pt–Ru anode electrocatalysts supported on multi-walled carbon nanotubes and their use in passive and active direct alcohol fuel cells with an anion-exchange membrane (alcohol= methanol, ethanol, glycerol). *Journal of Power Sources*, 190(2), pp.241-251.

8. Lamy, C., Belgsir, E.M. and Leger, J.M., 2001. Electrocatalytic oxidation of aliphatic alcohols: application to the direct alcohol fuel cell (DAFC). *Journal of Applied Electrochemistry*, 31(7), pp.799-809.
9. O'hayre, R., Cha, S.W., Prinz, F.B. and Colella, W., 2016. *Fuel cell fundamentals*. John Wiley & Sons.
10. Kordesch, K., Simander, G. and Besenhard, J.O., 1998. Fuel cells and their applications. *Angewandte Chemie-English Edition*, 37(9), p.1300.
11. Liu, H., Song, C., Zhang, L., Zhang, J., Wang, H. and Wilkinson, D.P., 2006. A review of anode catalysis in the direct methanol fuel cell. *Journal of Power Sources*, 155(2), pp.95-110.
12. Lamy, C., Léger, J.M. and Srinivasan, S., 2002. Direct methanol fuel cells: From a twentieth century electrochemists dream to a twenty-first century emerging technology. In *Modern aspects of electrochemistry* (pp. 53-118). Springer US.
13. Still looking for that article
14. Shen, S.Y., Zhao, T.S., Xu, J.B. and Li, Y.S., 2010. Synthesis of PdNi catalysts for the oxidation of ethanol in alkaline direct ethanol fuel cells. *Journal of Power Sources*, 195(4), pp.1001-1006.
15. Palma, L.M., Almeida, T.S. and De Andrade, A.R., 2013. high catalytic activity for glycerol electrooxidation by binary Pd-based nanoparticles in alkaline media. *ECS Transactions*, 58(1), pp.651-661.
16. Shen, P.K. and Xu, C., 2006. Alcohol oxidation on nanocrystalline oxide Pd/C promoted electrocatalysts. *Electrochemistry Communications*, 8(1), pp.184-188.
17. Coutanceau, C., Demarconnay, L., Lamy, C. and Léger, J.M., 2006. Development of electrocatalysts for solid alkaline fuel cell (SAFC). *Journal of Power Sources*, 156(1), pp.14-19.

18. Antolini, E., **2003**. Formation, microstructural characteristics and stability of carbon supported platinum catalysts for low temperature fuel cells. *Journal of materials science*, 38(14), pp.2995-3005.
19. Watanabe, M., Uchida, M. and Motoo, S., **1987**. Preparation of highly dispersed Pt+ Ru alloy clusters and the activity for the electrooxidation of methanol. *Journal of electroanalytical chemistry and interfacial electrochemistry*, 229(1-2), pp.395-406.
20. Aricò, A.S., Baglio, V., Di Blasi, A., Modica, E., Antonucci, P.L. and Antonucci, V., **2003**. Analysis of the high-temperature methanol oxidation behaviour at carbon-supported Pt–Ru catalysts. *Journal of Electroanalytical Chemistry*, 557, pp.167-176.
21. Di Blasia, A., Siracusano, S., Baglio, V., Briguglio, N., Brunaccina, G., Stasia, A., Ornelas, R., Antonucci, V. and Aricò, A.S., Investigation of a short stack PEM electrolyzer based on a nanosized IrO<sub>2</sub> anode electrocatalyst.
22. Yu, X. and Ye, S., **2007**. Recent advances in activity and durability enhancement of Pt/C catalytic cathode in PEMFC: Part I. Physico-chemical and electronic interaction between Pt and carbon support, and activity enhancement of Pt/C catalyst. *Journal of Power Sources*, 172(1), pp.133-144.
23. Ren, J., Ding, J., Chan, K.Y. and Wang, H., **2007**. Dual-porosity carbon templated from monosize mesoporous silica nanoparticles. *Chemistry of materials*, 19(11), pp.2786-2795.
24. Neto, A.O., Franco, E.G., Arico, E., Linardi, M. and Gonzalez, E.R., **2003**. Electro-oxidation of methanol and ethanol on Pt–Ru/C and Pt–Ru–Mo/C electrocatalysts prepared by Bönemann's method. *Journal of the European Ceramic Society*, 23(15), pp.2987-2992.
25. Hicks, T.T., **2004**. *Preparation, Characterization, and Activity of Mono-Dispersed Supported Catalysts* (Doctoral dissertation, Georgia Institute of Technology).

26. Xiong, L. and Manthiram, A., 2005. Nanostructured Pt–M/C (M= Fe and Co) catalysts prepared by a microemulsion method for oxygen reduction in proton exchange membrane fuel cells. *Electrochimica Acta*, 50(11), pp.2323-2329.
27. Swihart, M.T., 2003. Vapor-phase synthesis of nanoparticles. *Current Opinion in Colloid & Interface Science*, 8(1), pp.127-133.
28. Tsuji, M., Miyamae, N., Lim, S., Kimura, K., Zhang, X., Hikino, S. and Nishio, M., **2006**. Crystal structures and growth mechanisms of Au@ Ag core– shell nanoparticles prepared by the microwave– polyol method. *Crystal growth & design*, 6(8), pp.1801-1807.
29. Fievet, F., Lagier, J.P. and Figlarz, M., **1989**. Preparing monodisperse metal powders in micrometer and submicrometer sizes by the polyol process. *Mrs Bulletin*, 14(12), pp.29-34.
30. Song, K.C., Lee, S.M., Park, T.S. and Lee, B.S., **2009**. Preparation of colloidal silver nanoparticles by chemical reduction method. *Korean Journal of Chemical Engineering*, 26(1), pp.153-155.
31. Colmenares, L.C., Wurth, A., Jusys, Z. and Behm, R.J., 2009. Model study on the stability of carbon support materials under polymer electrolyte fuel cell cathode operation conditions. *Journal of Power Sources*, 190(1), pp.14-24.
32. Maass, S., Finsterwalder, F., Frank, G., Hartmann, R. and Merten, C., 2008. Carbon support oxidation in PEM fuel cell cathodes. *Journal of Power Sources*, 176(2), pp.444-451.
33. Qiao, Y., Li, C.M., Bao, S.J. and Bao, Q.L., 2007. Carbon nanotube/polyaniline composite as anode material for microbial fuel cells. *Journal of Power Sources*, 170(1), pp.79-84.

34. Shao, Y., Liu, J., Wang, Y. and Lin, Y., 2009. Novel catalyst support materials for PEM fuel cells: current status and future prospects. *Journal of Materials Chemistry*, 19(1), pp.46-59.
35. Rajalakshmi, N., Ryu, H., Shaijumon, M.M. and Ramaprabhu, S., 2005. Performance of polymer electrolyte membrane fuel cells with carbon nanotubes as oxygen reduction catalyst support material. *Journal of Power Sources*, 140(2), pp.250-257.



UNIVERSITY *of the*  
WESTERN CAPE

## CHAPTER 3: Experimental

### 3. Introduction

The chapter presents the details of the experimental and characterization methods employed in the synthesis and analysis of Pd, PdNi, PdNiO, PdMn<sub>3</sub>O<sub>4</sub>, PdMn<sub>3</sub>O<sub>4</sub>NiO all supported on multi-walled carbon nanotubes.

### 3.1 Chemicals

All chemicals used are listed in table 3.1. Ultrapure water from Millipore was used for all preparations.

Table 3.1: List of chemicals used for the study, and their suppliers.

Chemicals	Company
PdCl <sub>3</sub>	Alfa easar
NiCl <sub>3</sub>	Alfa easar
NiO	Sigma Aldrich
Mn <sub>3</sub> O <sub>4</sub>	Sigma Aldrich
EG	Kimix
KOH	Kimix
C <sub>3</sub> H <sub>8</sub> O	Kimix
C <sub>3</sub> H <sub>8</sub> O <sub>3</sub>	Kimix
C <sub>2</sub> H <sub>6</sub> O	Kimix
HNO <sub>3</sub>	Kimix
HCl	Sigma Aldrich
H <sub>2</sub> SO <sub>4</sub>	Kimix

Ultra-pure water	Milli-Q
MWCNT's	MWCNT company Japan

### 3.2 Methodology

This section discusses the detailed description of how the catalysts were prepared. Firstly, before the MWCNT were used they were treated with acid to remove impurities on their and to introduce on the surface of the MWCNTs functional groups known to be essential in enhancing catalyst loading and dispersing of the catalyst on the support.

#### 3.2.1 Pre-treatment of Carbon nanotubes

- The treatment was performed by using 5 g of Multi-walled carbon nanotubes treated in an aqueous solution composed of 90 ml concentrated sulphuric acid and 30 ml of concentrated nitric acid.
- The mixture was heated under reflux and stirring, with a water bath holding at 100°C for 3 hours.
- The mixture was then filtered, washed with ultra-pure water and dried overnight.

#### 3.2.2 Preparation of catalyst

All catalysts prepared in the study were prepared using the polyol method.

##### 3.2.2.1 Preparation of Pd/CNT

- A calculated mass of palladium chloride was dissolved in a 3:1 ratio of ethylene glycol and ultrapure water and stirred at room temperature to obtain a uniform mixture.

- To the uniform solution functionalised CNT particles were added and sonicated for 30 minutes.
- A solution of sodium borohydride with a concentration of  $1\text{mol.dm}^{-3}$  was slowly added to the mixture under vigorous stirring for 4 hours.
- After the 4 hours of stirring, the mixture was filtered and washed with ultrapure water and then dried overnight.

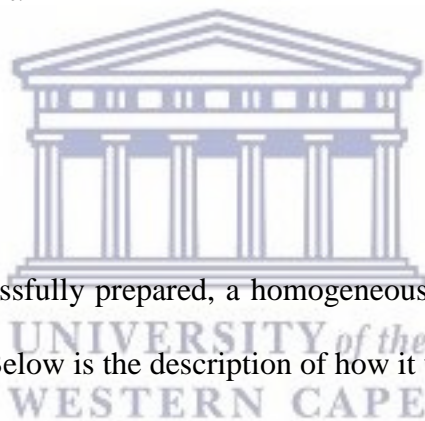
### 3.2.2.2 Preparation of binary catalyst (PdNi/CNT)

- A calculated mass of palladium chloride and nickel chloride (1:1 weight ratio) was dissolved in a 3:1 ratio of ethylene glycol and ultra-pure water and stirred at room temperature to obtain a uniform mixture.
- To the uniform solution functionalised CNT particles were added and sonicated for 30 minutes.
- A solution of sodium borohydride with a concentration of  $1\text{mol.dm}^{-3}$  was slowly added to the mixture under vigorous stirring for 4 hours.
- After the 4 hours of stirring, the mixture was filtered and washed with ultrapure water and then dried overnight.

All other binary catalysts; PdNiO and PdMn<sub>3</sub>O<sub>4</sub> were prepared in the same manner. The difference was the catalysts used to form a binary catalyst. For these other two binary catalysts nickel oxide and manganese oxide were used, respectively instead of nickel chloride.

### 3.2.2.3 Preparation of ternary catalyst (PdMn<sub>3</sub>O<sub>4</sub>NiO/CNT)

- A calculated mass of palladium chloride, nickel oxide and manganese oxide (1:1:1 weight ratio) was dissolved in a 3:1 ratio of ethylene glycol and ultra-pure water and stirred at room temperature to obtain a uniform mixture.
- To the uniform solution functionalised CNT particles were added and sonicated for 30 minutes.
- A solution of sodium borohydride with a concentration of 1mol.dm<sup>-3</sup> was slowly added to the mixture under vigorous stirring for 4 hours.
- After the 4 hours of stirring, the mixture was filtered and washed with ultrapure water and then dried overnight.



### 3.2.3 Preparation of ink

After the catalysts were successfully prepared, a homogeneous mixture of ink was prepared for electrochemical analysis. Below is the description of how it was prepared.

- 25mg of catalyst powder, 20 µL of nafion, 5 ml isopropanol and 4.15 mL ultrapure water were sonicated for 30 min.
- 5 ml of isopropanol was further added and the solution was sonicated for a further 1 and a half hour.

This was done for each of the five catalysts.

### 3.3 Characterization techniques

The physical, chemical and electrochemical properties of the prepared catalysts were studied using cyclic voltammetry, linear sweep voltammetry, Chronoamperometry, electrochemical impedance spectrometry, inductive coupled plasma – atomic emission spectroscopy, transmission electron microscopy, energy dispersion spectrometry and x-ray diffraction.

#### 3.3.1 Cyclic voltammetry

Cyclic voltammetry is probably the most versatile electro analytical technique for the study of electro active species. Its ease of measurement and versatility has resulted in it being in extensive use in many scientific fields like, electrochemistry, organic chemistry, inorganic chemistry and biochemistry. Cyclic voltammetry is usually the first technique performed in an electrochemical study of a compound, biochemical material or an electrode surface. The capability of cyclic voltammetry results from its ability to rapidly observe the redox reaction behaviour over a wide potential range. The resulting voltammograms is equivalent to a conventional spectrum in that it conveys information as a function of an energy scan [1].

In cyclic voltammetry the potential of a small, stationary working electrode is changed linearly with time starting from a potential where no electrode reaction occurs and moving to potentials where reduction or oxidation of a solute occurs. After going through the potential regions where one or more electrode reactions takes place, the direction of the linear sweep is reversed and the electrode reactions of the intermediates and products formed during the forward scan, often can be detected. The time scale of the experiment is controlled by the scan rate. Cyclic voltammetry is usually done using a three electrode system consisting of a working electrode, reference electrode and counter electrode in the presence of a supporting electrolyte. The reference electrode can be a standard hydrogen electrode, saturated calomel

electrode or silver electrode chloride. Counter electrodes can be gold, platinum or carbon while the working electrode is normally a glassy carbon electrode deposited with the catalyst being studied. The supporting electrolyte is present to repress migration of charged reactants and products [2]. It is typically used to characterize electrolytic activity in more detail.

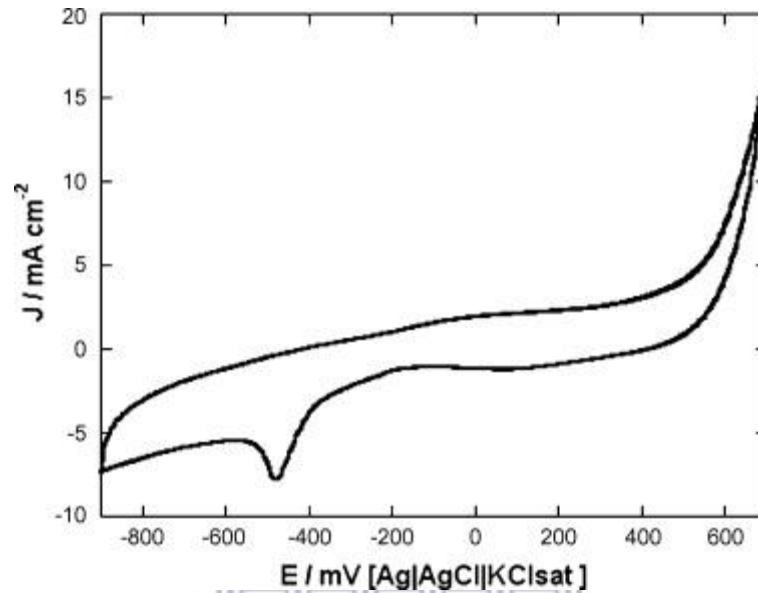


Figure 3.1 cyclic voltammogram of Pd/MWCNT (at the fifth cycle) in 2 M KOH solution. Pd loading  $17 \mu\text{g cm}^{-2}$ . Scan rate:  $50 \text{ mV s}^{-1}$ . [3]

The Pd reduction peak is used to calculate the electro-active surface area (ECSA). ECSA is a property which is used to determine the electro-catalytic activity of the prepared catalyst. The ECSA is an indication of the electro-active surface of the catalyst, calculated by using the equation:

$$ECSA(\text{m}^2 \text{ g}^{-1}_{Pd}) = [Q_H / 420 \cdot L \cdot A_g] 10^5$$

$Q_H$  = is the area of the Pd reduction peak divided by the scan rate,  $420 \mu\text{C cm}^{-2}$  is required to charge the formation of a monolayer of  $\text{H}_2$  on a smooth palladium surface.  $L$  is the loading of catalyst in  $\text{mg}_{Pd} \text{ cm}^{-2}$  and  $A_g$  the geometric surface area of the electrode (5 mm in diameter,  $A_g = 0.196 \text{ cm}^2$ ) [4, 5].

Table 3.2 Sample preparation and operating parameters for CV

Parameter	Specification
Electrolyte	Potassium hydroxide
Alcohol oxidation	n/a
Working electrode	Glassy carbon electrode
Counter electrode	Platinum electrode
Reference electrode	Silver chloride electrode
Scan rate	30 mV/s
Scan range	-0.9 – 0.3V



### 3.3.2 Linear sweep voltammetry

Linear sweep voltammetry is a voltammetric method where the current at a working electrode is measured while the potential between the working electrode and a reference electrode is swept linearly in time. Oxidation or reduction of species is registered as a peak or trough in the current signal at the potential at which the species begins to be oxidized or reduced [6]. The linear sweep voltammetry was used to determine the current density and onset potential of the catalysts for alcohol oxidation.

Table 3.3: Sample preparation and operating parameters for LSV

Parameter	Specification
Electrolyte	Potassium hydroxide
Alcohol oxidation	Ethanol or glycerol
Working electrode	Glassy carbon electrode
Counter electrode	Platinum electrode
Reference electrode	Silver chloride electrode
Scan rate	30 mV/s
Scan range	-0.9 – 0.3V

### 3.3.3 Chronoamperometry

In chronoamperometry the potential of the working electrode is stepped and the resulting current faradaic processes are monitored. Chronoamperometry is an electrochemical technique that generates high charging currents, which decay exponentially with time with time as any RC circuit. The faradaic current which is due to electron transfer is almost always the factor of interest [7]. In this work the Chronoamperometry was used to determine the stability of the catalysts.

Table 3.4: Sample preparation and operating parameters for chronoamperometry

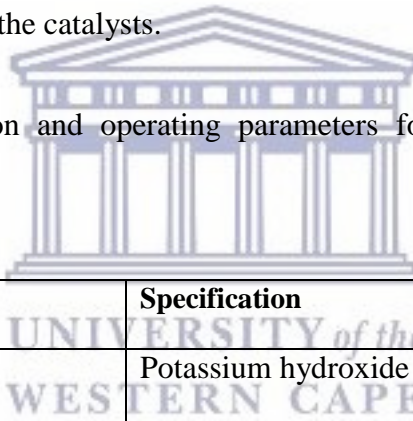
Parameter	Specification
Electrolyte	Potassium hydroxide
Alcohol oxidation	Ethanol or glycerol
Working electrode	Glassy carbon electrode
Counter electrode	Platinum electrode
Reference electrode	Silver/silver chloride electrode
Set potential	-0.2 V

### 3.3.4 Electrochemical Impedance spectroscopy

The resistance that a circuit has to a current when a voltage is applied is known as the impedance. Impedance is the complex ratio of the voltage to the current in an alternating current (AC) circuit. Unlike resistance, impedance possesses both phase and magnitude, while resistance possesses only the latter. Resistance can be viewed as impedance with zero phase angles. When a circuit is driven with a direct current, there is no differentiating between impedance and resistance.

The symbol for impedance is usually  $Z$  and it may be represented by writing its magnitude and phase in the form  $|Z|\angle\theta$  [8]. The electrochemical impedance spectroscopy was used to study the electrode kinetics of the catalysts.

Table 3.5: Sample preparation and operating parameters for electrochemical impedance spectrometry



Parameter	Specification
Electrolyte	Potassium hydroxide
Alcohol oxidation	Ethanol or glycerol
Working electrode	Glassy carbon electrode
Counter electrode	Platinum electrode
Reference electrode	Silver chloride electrode
Set potential	-0.1 or -0.3 V

### 3.3.5 Inductively coupled plasma – atomic emission spectroscopy

Inductive coupled plasma – atomic emission spectroscopy is an analytical technique used to detect traces of metals in a sample. It is a type of emission spectroscopy that uses the inductive coupled plasma to produce excited atoms and ions that emit electromagnetic radiation at wavelengths characteristic of a particular element. It is a flame technique with a flame ranging from 6000 to 10000 K. The intensity of this emission is indicative of the concentration of the element within the sample [9].

A Thermo Icap 6300 ICP-AES spectrometer was used to measure the concentrations of Pd, Ni, NiO and Mn<sub>3</sub>O<sub>4</sub> using the general ICP conditions. For the determination of metal loadings 40-50 mg of all the catalysts of interest were decomposed by aqua regia (3HCl: 1HNO<sub>3</sub>) and diluted with water to a total volume of 50 ml. After filtration of the residual carbon nanotube support, the samples were analysed by ICP-AES. Standards were matrix matched to acid concentration of samples. After calibration and quality check analysis to verify accuracy of standards, samples were analysed without dilution.

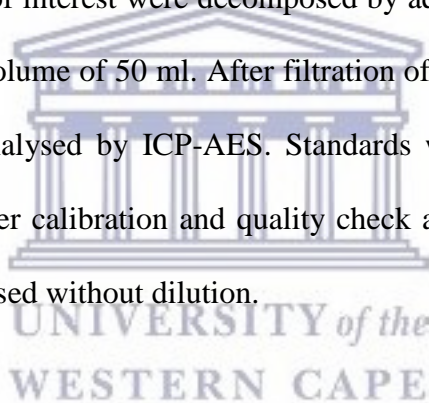


Table 3.6: ICP operating conditions for determination of Pd, Ni and Mn

Parameter	Setting
Generator power	1300 W
View mode	Radial
View height	15mm
Plasma	Argon
Shear gas	Argon
Gas flow: plasma	15 ml.min <sup>-1</sup>
Gas flow: auxiliary	1.5 ml.min <sup>-1</sup>
Gas flow: nebulizer	1.5 ml.min <sup>-1</sup>
Sample aspiration\rate	2 ml.min <sup>-1</sup>
Detector	PMT
Emission line: Pd	340.458 nm
Emission line: Ni	231.604 nm and 221.648 nm
Emission line: Mn	257.610 nm
Rinse delay	15 s
Read	Peak area
Replicate read time	2 s
Number of replicates	3

### **3.3.6 Transmission electron microscopy**

Optical microscopes have a limited ability to resolve some object because of its wavelength. Transmission electron microscopes (TEM) were developed to obtain magnification and details of a specimen at a much better level compared to conventional microscopes. The development of TEM took into consideration the quantum mechanical behaviour of electrons. The interaction of electrons with the material was obtained due to the inherent nature of electron which is a quantum mechanical object. Due to the electrons having both wave and particle nature and the de Broglie wavelength of electrons are significantly smaller than that of light and so they higher resolution capability. This enables the finer detail examination, to even as small as a single column of atoms. A single column of atoms is tens of thousands times smaller than the smallest resolvable object in a light microscope.

The transmission of electron beam is highly dependent on the properties of material being examined. Such properties include density and composition. For example a porous material will allow more electrons to pass through while dense material will allow less. This results in a specimen with a non-uniform density being able to be examined by this technique [10, 11].

#### **Sample preparation**

A spatula tip of powdered sample is suspended in ethanol in a vial. The mixture is then sonicated for 10 minutes to ensure efficient dispersion. A micro pipette is then used to extract some of the sample from the solution which is drop coated on a 400 mesh copper grid. The copper grid is then left to air dry under a lamp for 10 minutes. The sample is then placed in the sample tray for analysis.

### **Instrument setup:**

HR-TEM Technai G2 F20 X-Twin MAT 200 kV Field Emission Transmission Electron Microscope

Table 3.7: operating conditions for HR-TEM

<b>Parameter</b>	<b>Setting</b>
Gunlens used	Gunlens 1
Spot size	3
Objective aperture	1
Accelerating voltage	200 Kv

### **3.3.7 Energy dispersion spectroscopic analysis (EDS) in scanning electron microscope (SEM)**

Energy dispersive X-Ray spectroscopy (EDS or EDX) was used to determine the elemental composition of Pd, Ni and Mn in the respective electro-catalysts synthesized and also to confirm the structural formation of Pd, Ni and Mn on the catalyst support. EDS analysis was performed on a HR-SEM. The incident electron energies were kept constant at 10 keV for all the samples.

### 3.3.8 X-ray diffraction

The discovery of X-rays enabled scientists to probe crystalline structure at the atomic level. X-ray diffraction has been in use in two main areas, for the fingerprint characterization of crystalline materials and determination of their structure. Each crystalline solid has its unique characteristic X-ray powder pattern which may be used as a fingerprint for its identification. Once the material has been identified, X-ray crystallography may be used to determine its structure, and that is how the atoms pack together in the crystalline state, and what the interatomic distance and angle are. X-ray diffraction is one of the most important characterization tools used in solid state chemistry and materials science [12]. We can determine size and shape of the unit cell for any compound most easily using X-ray diffraction.

The structural properties of the electro-catalysts were investigated using XRD. From the obtained results the average crystallite size, ( $\langle D \rangle$ , Å) was calculated from line broadening analysis using the Scherrer formula. The Scherrer equation was used as shown in Equation to estimate the crystallite size from the XRD data [12]

$$d = \frac{0.9\lambda}{\beta \cos \theta}$$

Where  $d$  = crystallite size,  $0.9$  = shape factor,  $\lambda$  = x-ray wavelength,  $\beta$  = peak width at half peak height and  $\theta$  = angle of reflection

**Instrument setup:**

**Manufacturer:** BRUKER AXS (Germany), **Diffractometer:** D8 Advance

**Tube:** Cu-K $\alpha$  radiation ( $\lambda_{K\alpha 1}=1.5406\text{\AA}$ )

**Detectors:** PSD Vantec-1, Gas detector with 1600 channels

Table 3.8: operating conditions for X-ray diffractometer.

Parameters	Settings
Tube voltage	40Kv
Tube current	40 mA
Variable slits	0.28 mm
2 $\theta$ Range	0-90 (angle in degrees)
Increment	$\Delta 2\theta$ : 0.048 deg
Measurement time	1 sec

### 3.4 References

1. Nicholson, R.S., 1965. Theory and Application of Cyclic Voltammetry for Measurement of Electrode Reaction Kinetics. *Analytical Chemistry*, 37(11), pp.1351-1355.
2. Evans, D.H., O'Connell, K.M., Petersen, R.A. and Kelly, M.J., 1983. Cyclic voltammetry.
3. Bambagioni, V., Bianchini, C., Marchionni, A., Filippi, J., Vizza, F., Teddy, J., Serp, P. and Zhiani, M., 2009. Pd and Pt–Ru anode electrocatalysts supported on multi-walled carbon nanotubes and their use in passive and active direct alcohol fuel cells with an anion-exchange membrane (alcohol= methanol, ethanol, glycerol). *Journal of Power Sources*, 190(2), pp.241-251.
4. Grdeń, M., Łukaszewski, M., Jerkiewicz, G. and Czerwiński, A., 2008. Electrochemical behaviour of palladium electrode: oxidation, electrodisolution and ionic adsorption. *Electrochimica Acta*, 53(26), pp.7583-7598.
5. Bard, A.J. and Faulkner, L.R., 2001. Fundamentals and applications. *Electrochemical Methods*, 2.
6. Osteryoung, J., linear sweep voltammetry at very small stationary disk electrodes.
7. [http://www.asdlib.org/onlineArticles/ecourseware/Kelly\\_Potentiometry/PDF-6-Chronoamp.pdf](http://www.asdlib.org/onlineArticles/ecourseware/Kelly_Potentiometry/PDF-6-Chronoamp.pdf)
8. <http://bmia.bmt.tue.nl/people/BRomeny/Courses/8C120/pdf/ElectricalImpedance.pdf>
9. [https://en.wikipedia.org/wiki/Inductively\\_coupled\\_plasma\\_atomic\\_emission\\_spectroscopy](https://en.wikipedia.org/wiki/Inductively_coupled_plasma_atomic_emission_spectroscopy)
10. [https://en.wikipedia.org/wiki/Transmission\\_electron\\_microscopy](https://en.wikipedia.org/wiki/Transmission_electron_microscopy)
11. Reimer, L., 2013. *Transmission electron microscopy: physics of image formation and microanalysis* (Vol. 36). Springer.

12. [http://en.wikipedia.org/wiki/Energy-dispersive\\_X-ray\\_spectroscopy](http://en.wikipedia.org/wiki/Energy-dispersive_X-ray_spectroscopy)



UNIVERSITY *of the*  
WESTERN CAPE

## CHAPTER 4: Results and discussion

### 4. Chapter overview

The results and discussion of this chapter start with physical characterization to check morphology and particle size using high resolution transmission electron microscopy (HR-TEM) and X-ray diffraction was used to check crystalline size or average particle size. The electrochemical characterization was performed using cyclic voltammetry, linear sweep voltammetry, electrochemical impedance spectroscopy and chronoamperometry to check for the catalyst electro-activity.



### 4.1 Physical properties

Table 4.1: values of particle size and metal loading for the in-house catalysts.

Catalyst	Average particle size XRD (nm)	Particle size HR-TEM (nm)	Pd loading (wt. %)	Ni loading (wt. %)	Mn loading (wt. %)
Pd	1.41	5.18	19.38	-	-
PdNi	0.97	5.05	16.25	5.25	-
PdNiO	2.69	3.44	16.03	6.23	-
PdMn <sub>3</sub> O <sub>4</sub>	1.06	5.29	15.47	-	7.25
PdMn <sub>3</sub> O <sub>4</sub> NiO	1.25	7.20	13.89	4.26	5.65

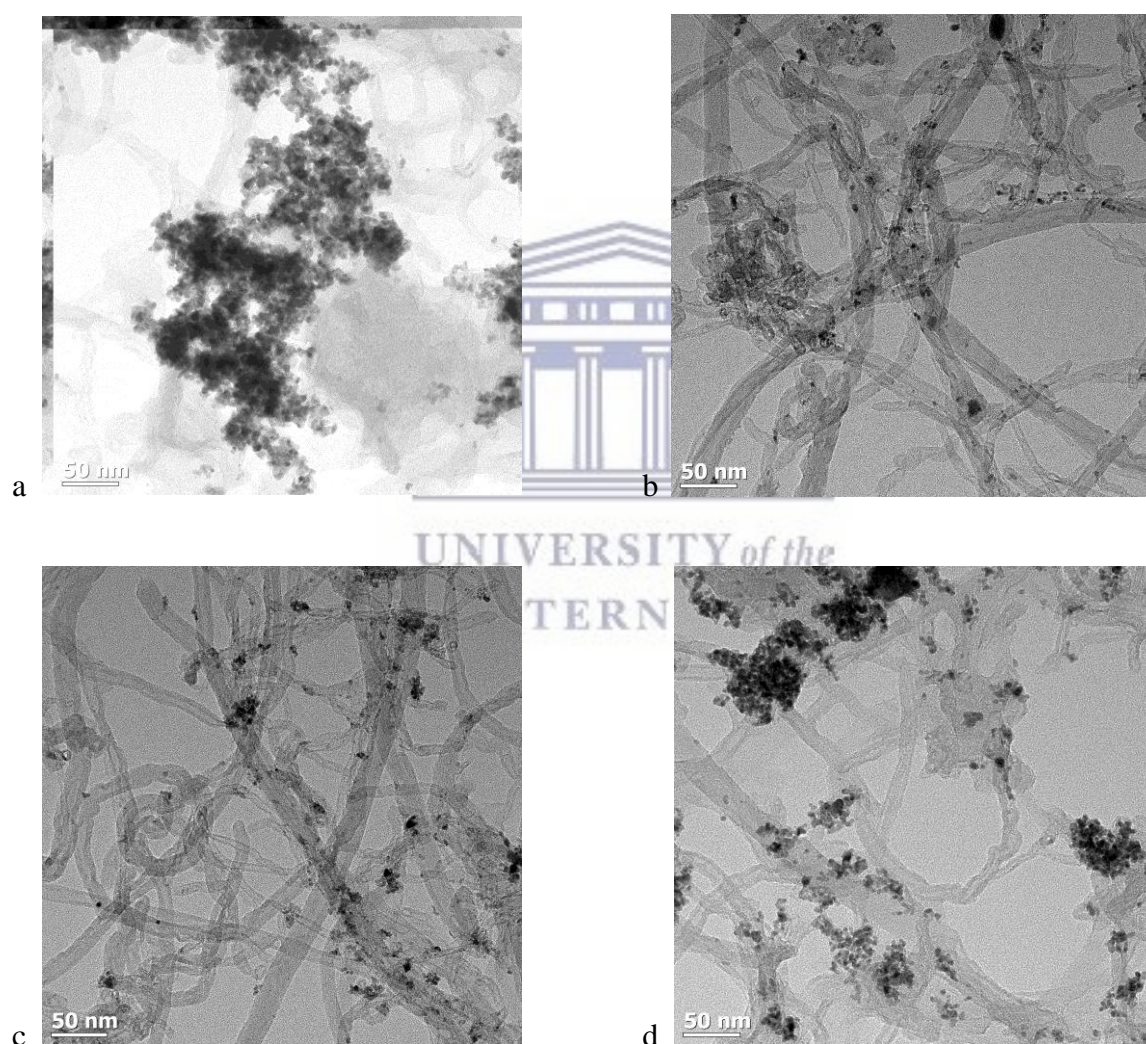
The average particle size for the in house catalyst in this research calculated from the Pd (220) diffraction peak is observed to be; 1.41 nm Pd, 0.97 nm PdNi, 2.69 nm PdNiO, 1.06 nm PdMn<sub>3</sub>O<sub>4</sub> and 1.25 nm PdMn<sub>3</sub>O<sub>4</sub>NiO. PdNi had the smallest average particle size from all in house catalysts. The particle size observed from the HR-tem for the in house catalysts shows PdNiO having the smallest particles size at 2.69 nm while it showed the largest average particle size.

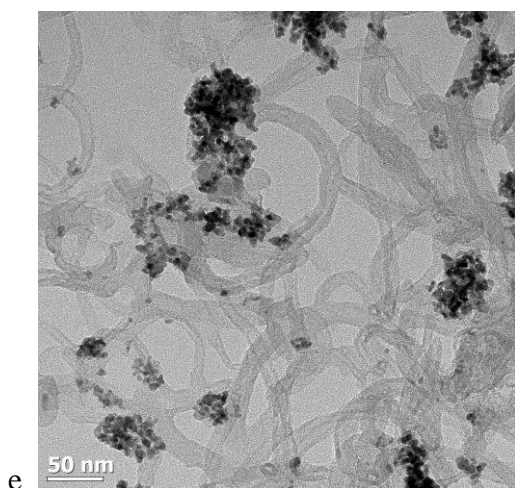
The total catalyst loading for the in house catalysts is observed to be close to 20% catalysts loading for all the five catalysts.



## 4.2 HR-TEM analysis

Below is the TEM images of the in-house catalysts supported on MWCNTs. The HRTEM images of the catalysts in figure 4.28 a) Pd, b) PdNi, c) PdNiO, d) PdMn<sub>3</sub>O<sub>4</sub> e) PdMn<sub>3</sub>O<sub>4</sub>NiO show that some of the catalysts were agglomerated with irregular shapes. Images b and c showed the best dispersion of the catalyst on the support material.

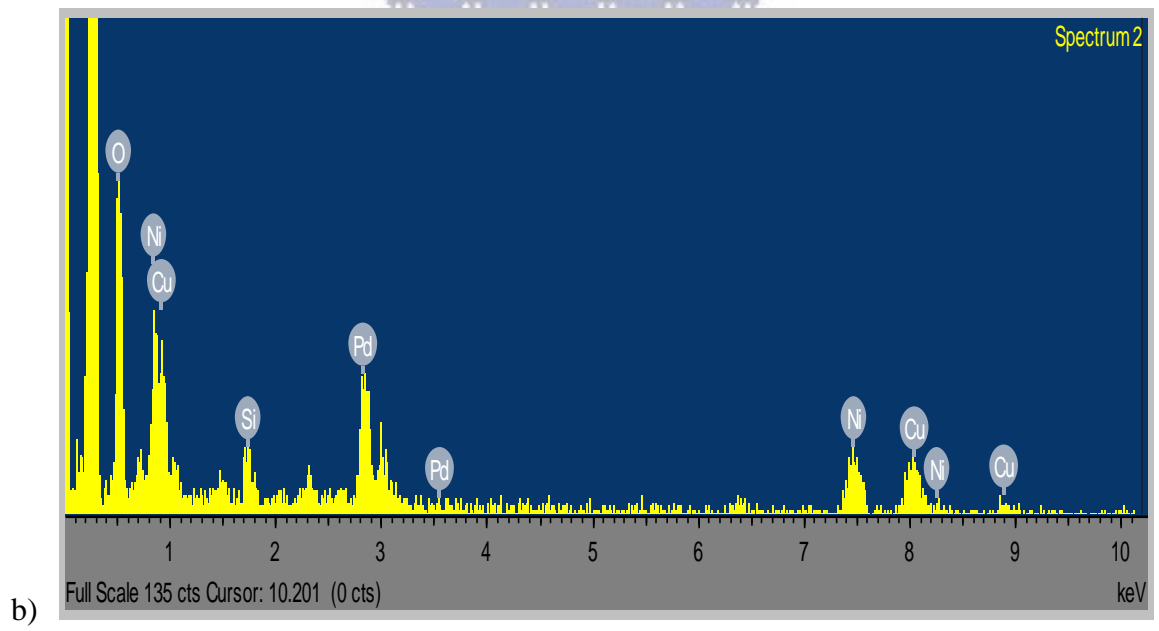
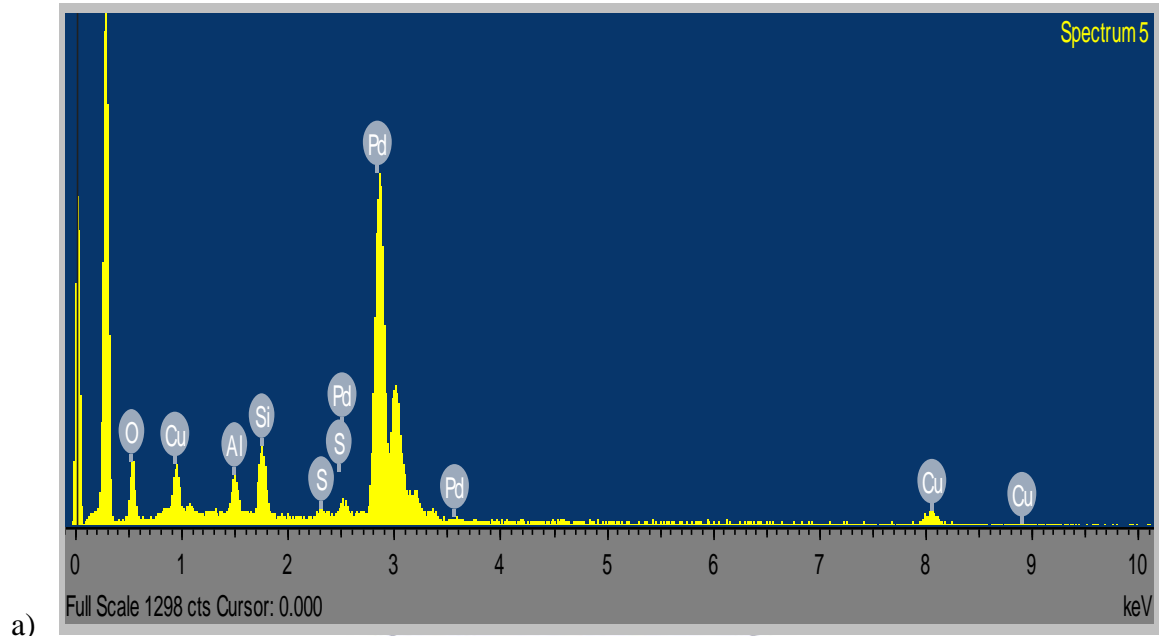


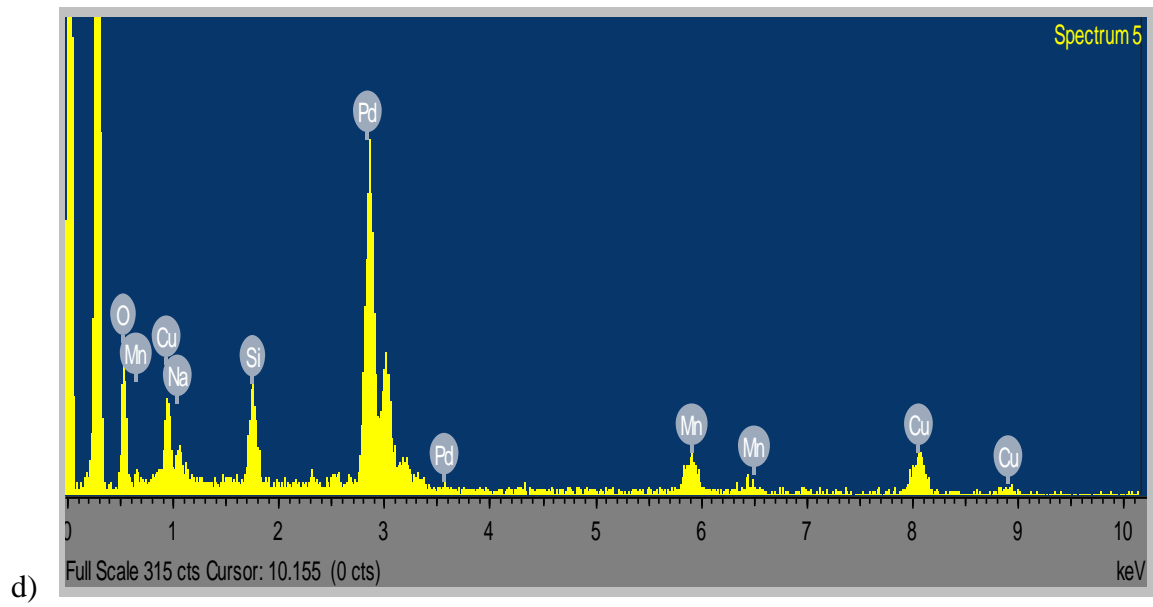
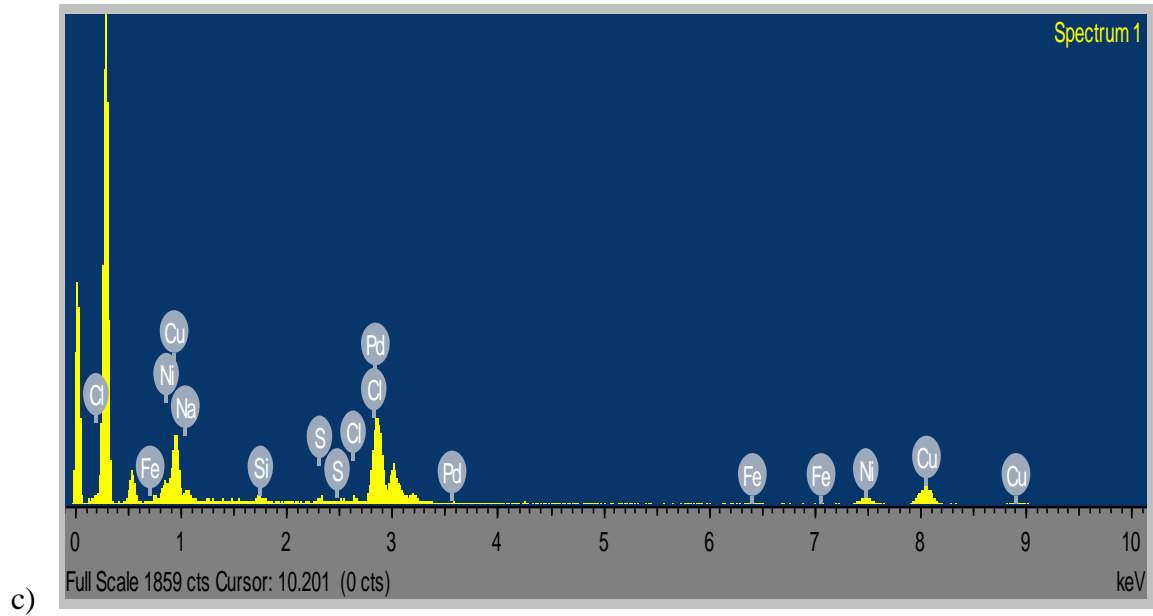


*Figure 4.1 HRTEM images of a)Pd ,b) PdNi,c) PdNiO,d) PdMn3O4 and e)PdMn3O4NiO in-house electro-catalysts on MWCNT*

The HR-TEM images of the catalyst in figure show that there is not much agglomeration of the catalysts. Images b and c show the best catalyst dispersion on the catalyst support material. The two catalysts b (PdNi) and c (PdNiO) showed the best performance in ethanol. The ternary catalysts i.e catalyst e and the mono-catalyst i.e catalyst a, were the most agglomerated catalysts. The particle size was obtained for each catalyst and it was observed the two least agglomerated catalysts gave the smallest particle sizes. PdNiO was the best performing catalyst in both alcohols and this catalyst had the smallest particle size. Both catalysts with  $Mn_3O_4$  gave larger particle sizes compared to Pd, PdNi and PdNiO which do not contain the metal oxide  $Mn_3O_4$ . The mono-catalyst Pd even though it had a smaller particle size compared to PdMn<sub>3</sub>O<sub>4</sub> and PdMn<sub>3</sub>O<sub>4</sub>NiO it was the least active and least stable catalyst from the five in-house

### 4.3 EDS analysis





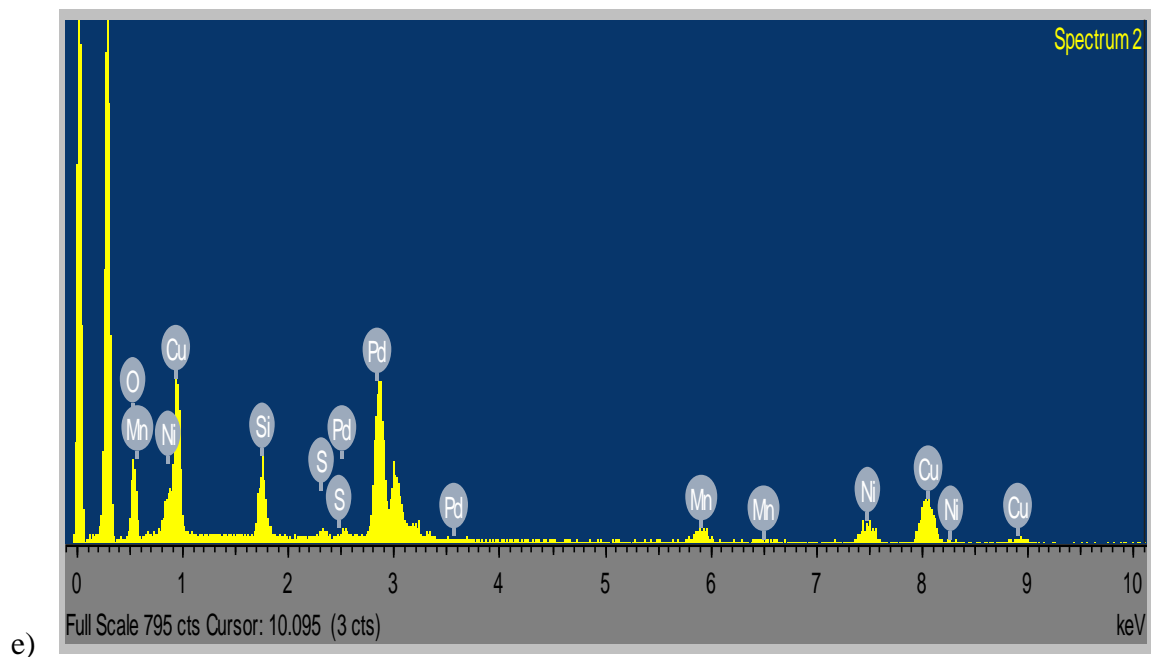


Figure 4.2: EDX spectra of a) Pd, b) PdNi, c) PdNiO d) PdMn<sub>3</sub>O<sub>4</sub>, e) PdMn<sub>3</sub>O<sub>4</sub>NiO in-house electro-catalyst on MWCNT support

The elemental analysis was conducted to study the elemental composition of the in-house catalysts. Figure 4.3, shows the EDX spectra of the in-house catalysts confirms the presence of the elements in the prepared catalysts. The elemental composition was performed on a HR-SEM.

#### 4.4 X-ray diffraction analysis

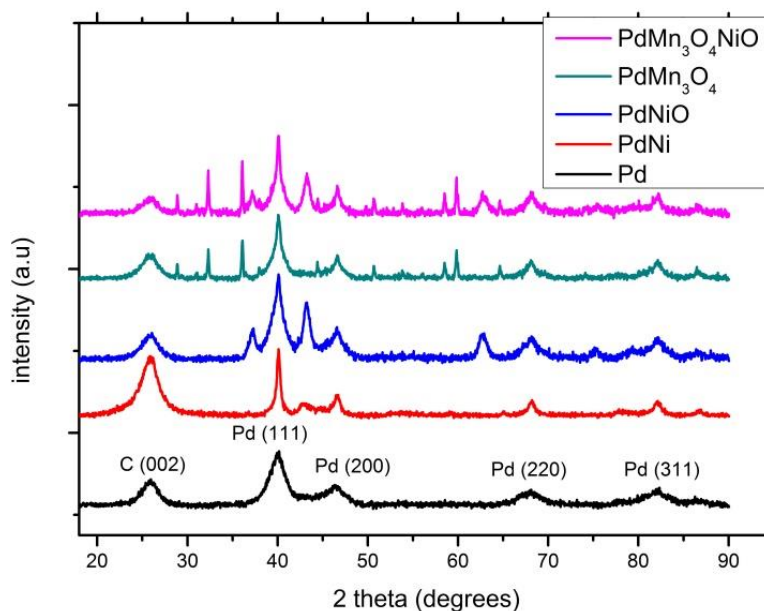


Figure 4.3 x-ray diffraction of 20% Pd, PdNi, PdMn, PdNiO, PdMn<sub>3</sub>O<sub>4</sub> and PdMn<sub>3</sub>O<sub>4</sub>NiO in-house electro-catalysts on MWCNT support

The XRD patterns for the in-house catalysts are presented in figure 4.4 above. The strongest and sharpest diffraction peak for all five samples is at around  $2\theta = 40.05^\circ$  which could be indexed as (111) reflection of Pd, and the other characteristic Pd diffraction peaks at  $2\theta$  of about  $47.05^\circ$ ,  $67.95^\circ$  and  $82.10^\circ$  corresponded to (200), (220) and (310), respectively [5]. The diffraction peak for carbon attributed by the MWCNTs at about  $2\theta = 25^\circ$  which corresponds to (002) is one of the five major peaks including the four from Pd. The diffraction peaks were all observed at the same  $2\theta$  values for all the in-house catalysts showing no significant shift showing the Pd and the metal oxides did not alloy well with this preparation method. The combined XRD patterns for PdNiO, PdMn<sub>3</sub>O<sub>4</sub> and PdMn<sub>3</sub>O<sub>4</sub>NiO show the peaks for the Pd peaks and also show the diffraction peaks for the metal oxides and these shows that they coexist in the sample. The average size of the metal particles is calculated based on the

broadening of the (220) diffraction peak according to Scherrer's equation. From table 4.4 the particle size can be seen with PdNi showing the smallest particle size of 0.92 nm.



## 4.5 Cyclic voltammetry study

The figure below shows the oxidation reduction reactions of the prepared catalysts.

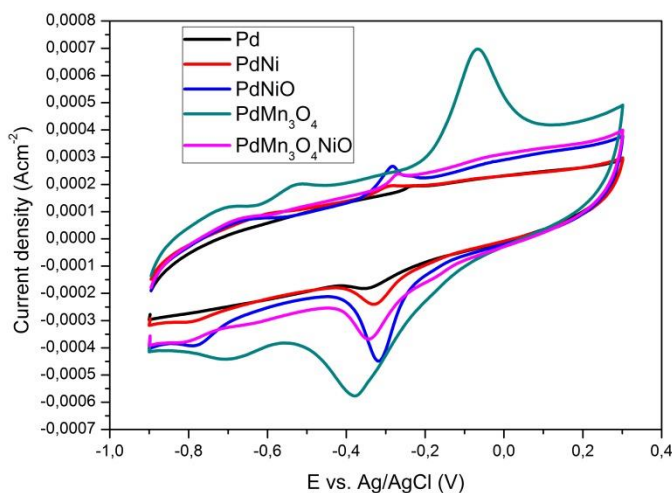


Figure 4.4 Cyclic voltammetry of Pd, PdNi, PdMn, PdNiO, PdMn<sub>3</sub>O<sub>4</sub> and PdMn<sub>3</sub>O<sub>4</sub>NiO in-house electro-catalysts on MWCNT support in N<sub>2</sub> saturated 1.0M KOH at a scan rate of 30mV.s<sup>-1</sup>

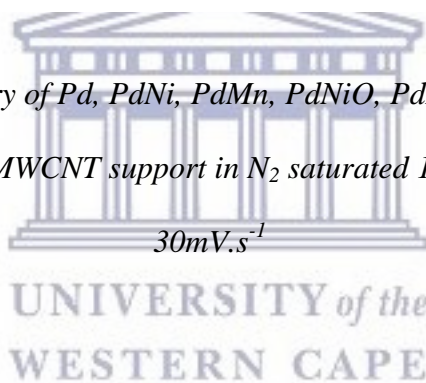


Figure 4.4 is the cyclic voltammetry of Pd, PdNi, PdNiO, PdMn<sub>3</sub>O<sub>4</sub> and PdMn<sub>3</sub>O<sub>4</sub>NiO in-house electro-catalysts on MWCNT. From the voltammogram the oxidation peaks for the different catalysts can be observed. The oxidation peak was observed at -0.25V for Pd and this was the least intense reduction peak observed for the in-house catalysts. PdMn<sub>3</sub>O<sub>4</sub> showed the most intense peaks for the oxidation and reduction compared to the other in-house catalysts. The oxidation peak was observed at -0.2V for PdMn<sub>3</sub>O<sub>4</sub> and the reduction peak was observed at 0.01V. The peak area of the oxidation peak in the cyclic voltammetry was used to determine the electro-active surface area of the catalysts using;

$$ECSA(m^2/g) = [Q_H(C/cm^2) / 420 \mu C cm^{-2} \cdot LPd(mgPd.cm^{-2}) \cdot Ag(cm^2)] 10^5$$

Table 4.2 below shows ECSA of the in-house catalysts. With the decrease in the particle size, the value for the ECSA increases. This trend is observed in this study for the binary and the ternary catalysts, however an abnormality was observed for PdMn<sub>3</sub>O<sub>4</sub> where it does not have the smallest particle size, but it has the highest ECSA value

*Table 4.2 ECSA values of Pd, PdNi, PdNiO, PdMn<sub>3</sub>O<sub>4</sub> and PdMn<sub>3</sub>O<sub>4</sub>NiO in-house electro-catalysts on MWCNT*

Catalyst	ECSA (m <sup>2</sup> g <sup>-1</sup> <sub>Pd</sub> )
Pd	14.43
PdNi	16.29
PdNiO	31.39
PdMn <sub>3</sub> O <sub>4</sub>	61.45
PdMn <sub>3</sub> O <sub>4</sub> NiO	27.11

UNIVERSITY of the  
WESTERN CAPE

#### 4.6 Linear sweep voltammetry study

The figures below compare the activity of the prepared catalysts towards ethanol and glycerol.

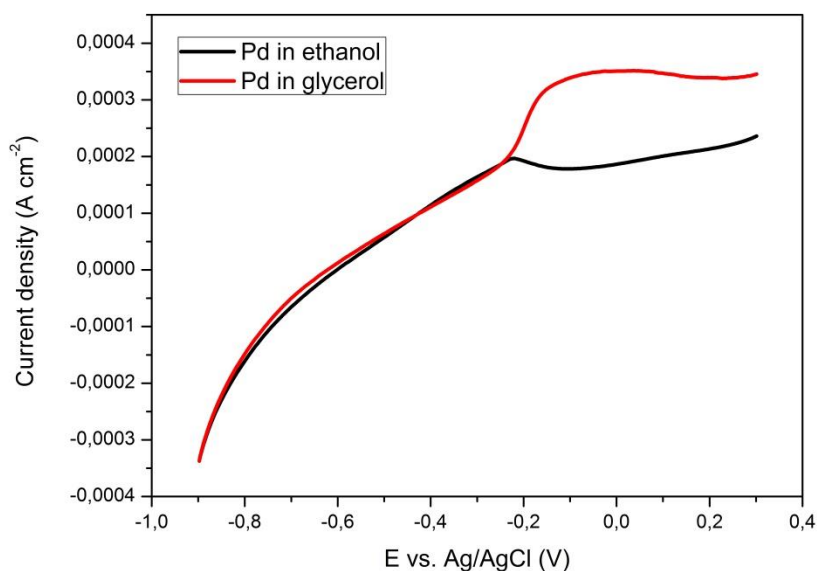
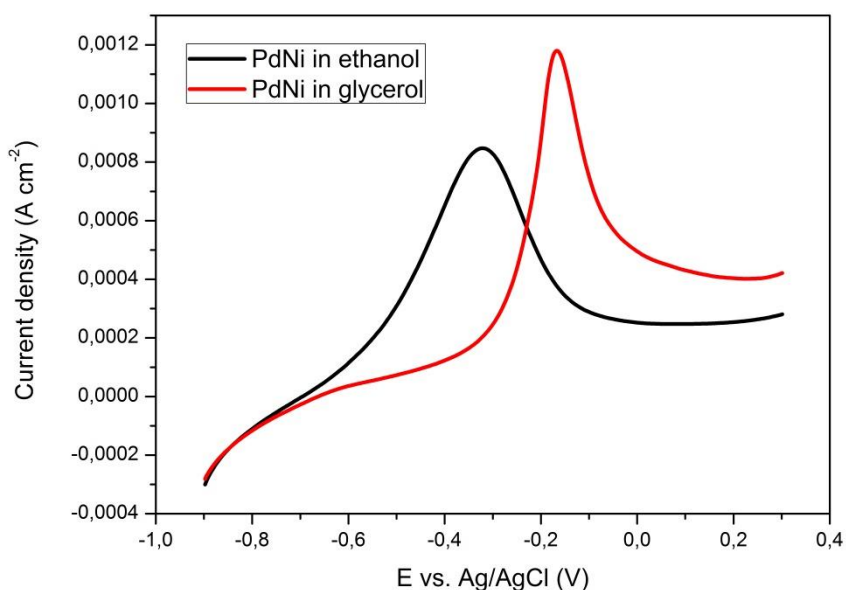


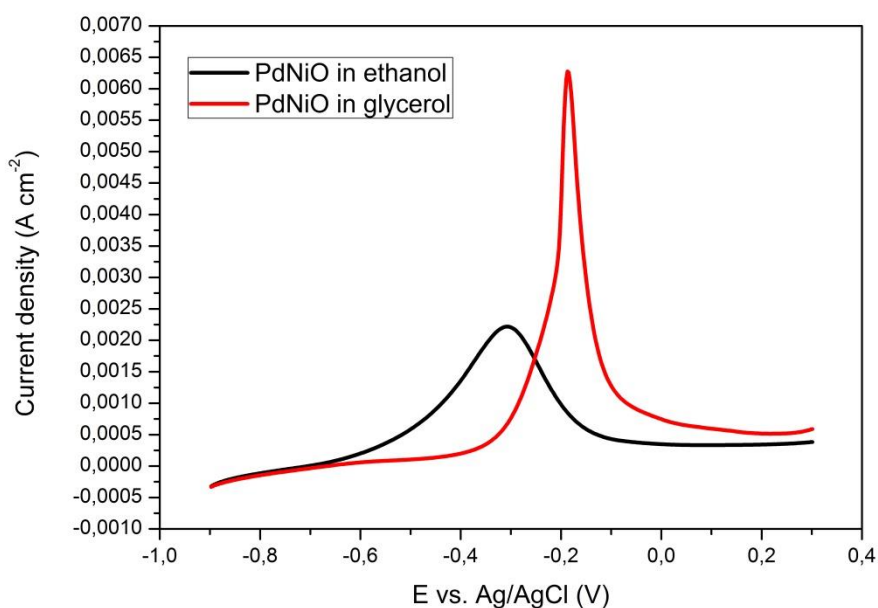
Figure 4.5 Linear sweep voltammetry of Pd in-house electro-catalysts on MWCNT support in N<sub>2</sub> saturated 1.0M KOH comparing the activity in 1M ethanol and 1M glycerol at a scan rate of 30mV.s<sup>-1</sup>

Figure 4.5 shows the LSV for Pd supported on MWCNTs, a higher current density towards glycerol oxidations is observed compared to ethanol oxidation. A current density of 0.20 mAcm<sup>-2</sup> was observed for the Pd catalyst in ethanol, while a current density of 0.35 mAcm<sup>-2</sup> is observed for glycerol. The catalyst onset potential observed at -0.25 V appears to be the same in both alcohols.



*Figure 4.6 Linear sweep voltammetry of PdNi in-house electro-catalysts on MWCNT support in N<sub>2</sub> saturated 1.0M KOH comparing the activity in 1M ethanol and 1M glycerol at a scan rate of 30mV.s<sup>-1</sup>*

The above figure, figure 4.6 shows an improvement in current density for PdNi supported on MWCNTs in both fuels compared to that observed in Pd. Like Pd, PdNi shows a higher current density in glycerol than in ethanol. A current density of 0.85 mAcm<sup>-2</sup> is observed in ethanol while glycerol gave a current density of 1.19 mAcm<sup>-2</sup>. An earlier onset potential of -0.66 V is observed in ethanol while for glycerol the onset potential for oxidation is -0.38 V.



*Figure 4.7 Linear sweep voltammetry of PdNiO in-house electro-catalysts on MWCNT support in N<sub>2</sub> saturated 1.0M KOH comparing the activity in 1M ethanol and 1M glycerol at a scan rate of 30mV.s<sup>-1</sup>*

Figure 4.7 shows a huge difference for current density observed for PdNiO using the two different alcohols. The catalysts shows a higher current density for glycerol which is 6.25 mAcm<sup>-2</sup> compared to 2.25 mAcm<sup>-2</sup> observed for ethanol. An onset potential was observed to be -0.68 V in ethanol, while for glycerol the onset potential was observed at -0.41 V.

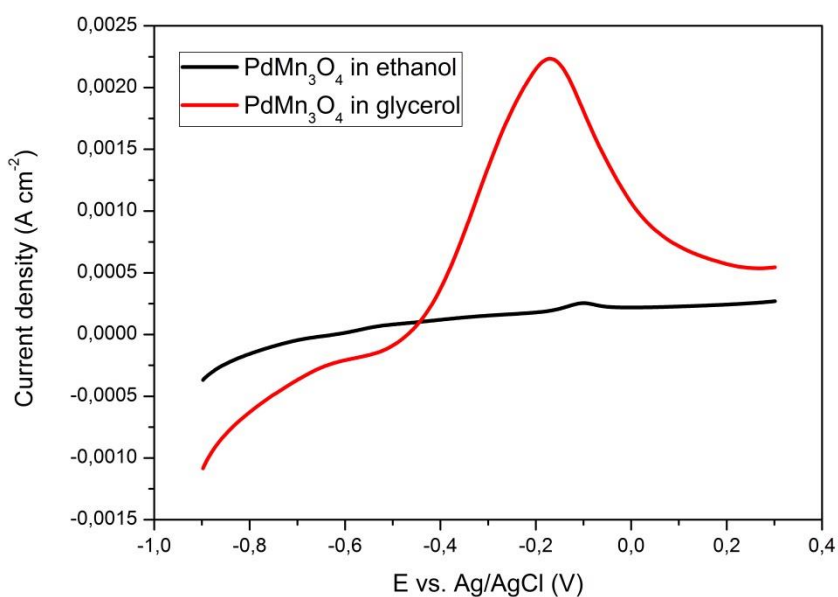


*Figure 4.8 Linear sweep voltammetry of PdMn<sub>3</sub>O<sub>4</sub> in-house electro-catalysts on MWCNT support in N<sub>2</sub> saturated 1.0M KOH comparing the activity in 1M ethanol and 1M glycerol at a scan rate of 30mV.s<sup>-1</sup>*

Figure 4.8 shows a LSV for PdMn<sub>3</sub>O<sub>4</sub> supported on MWCNTs. A higher current density is observed towards glycerol oxidation compared to that of ethanol oxidation. The current density is observed at 0.25 mAcm<sup>-2</sup> in the presence of ethanol, while for glycerol the current density is 2.25 mAcm<sup>-2</sup>. The onset potential is -0.51 V for the former while ethanol shows an onset potential at -0.18 V.

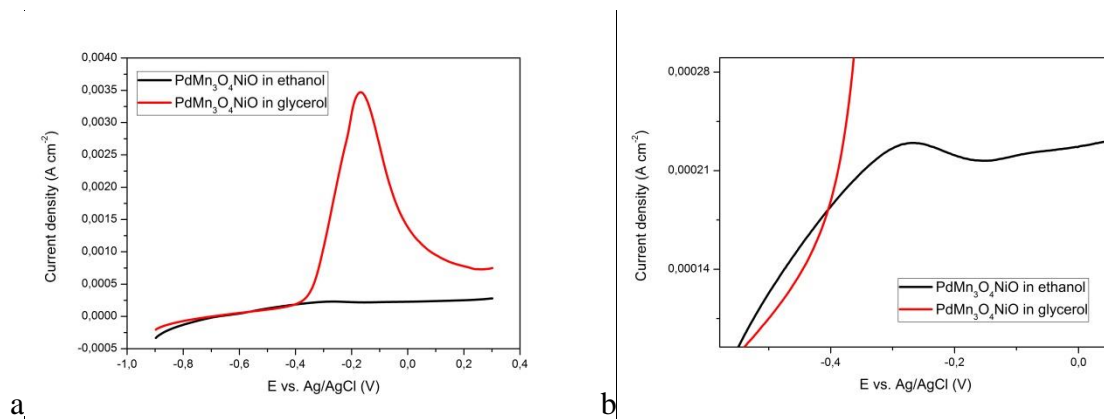
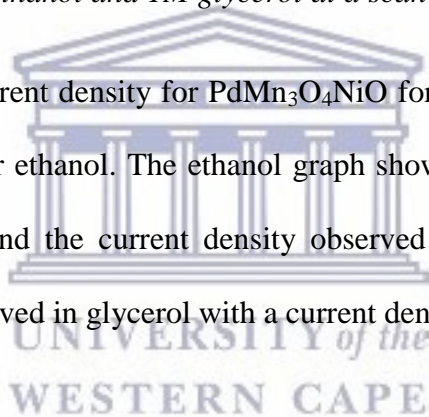


figure 4.9a) Linear sweep voltammetry of  $\text{PdMn}_3\text{O}_4\text{NiO}$  in-house electro-catalysts on MWCNT, Figure 4.9 b) shows a zoomed in figure of Linear sweep voltammetry of  $\text{PdMn}_3\text{O}_4\text{NiO}$  in-house electro-catalysts on MWCNT support in  $\text{N}_2$  saturated 1.0M KOH comparing the activity in 1M ethanol and 1M glycerol at a scan rate of  $30\text{mV}\cdot\text{s}^{-1}$

Figure 4.9 shows a higher current density for  $\text{PdMn}_3\text{O}_4\text{NiO}$  for glycerol oxidation. An early onset potential is observed for ethanol. The ethanol graph shows a steady increase from the start of the scan at -0.9 V and the current density observed is  $0.225\text{ mAcm}^{-2}$ . An onset potential of -0.39 V is observed in glycerol with a current density of  $3.49\text{ mAcm}^{-2}$ .



The figure below shows the LSV for the prepared in-house catalysts in ethanol

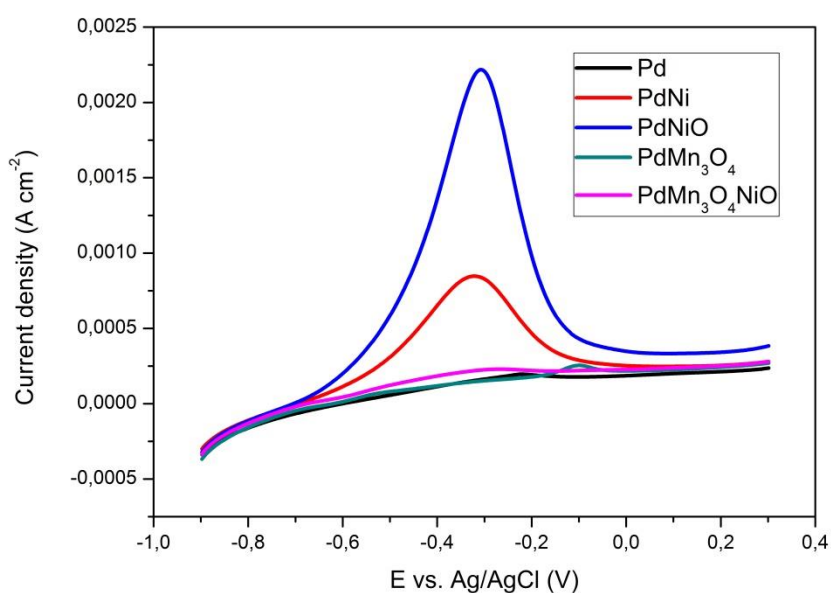


Figure 4.10 Linear sweep voltammetry of Pd, PdNi, PdNiO, PdMn<sub>3</sub>O<sub>4</sub> and PdMn<sub>3</sub>O<sub>4</sub>NiO in-house electro-catalysts on MWCNT support in N<sub>2</sub> saturated 1.0M KOH with 1.0M ethanol at a scan rate of 30mV.s<sup>-1</sup>

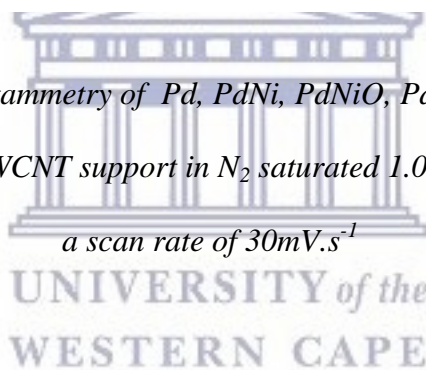
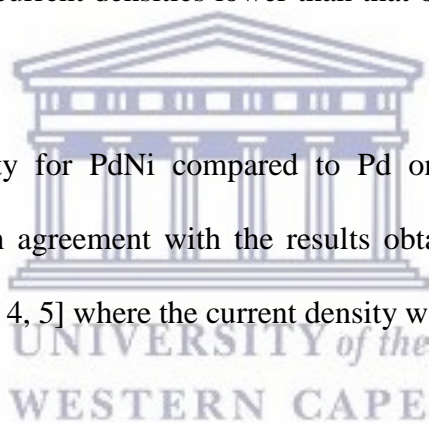


Figure 4.10 shows the combined linear sweep voltammetry of 20% Pd, PdNi, PdNiO, PdMn<sub>3</sub>O<sub>4</sub> and PdMn<sub>3</sub>O<sub>4</sub>NiO in-house electro-catalysts on MWCNT. The LSV's show the ethanol oxidation peaks for the five in-house catalysts. The LSV curves display the typical behaviour observed for EOR. It can be seen that by alloying the Pd catalyst with other metals an improved current density was obtained. PdNi and PdNiO were the two most active catalysts towards ethanol from the five in-house catalysts showing that nickel metal was the best alloy metal in this study. PdNiO shows the highest current density compared to the other catalysts. Table 4.3 shows the obtained onset potentials and current densities obtained for all catalysts towards ethanol oxidation. Xu et al. [1] believe it is possible that oxides function as

Ru does for Pt, in Pd-oxide support on carbon materials, because the OH<sub>ad</sub> species could also form on the surface of the oxide. The formation of OH<sub>ad</sub> species at lower potentials can transform CO-like or other carbonaceous species on the surface of Pd to CO<sub>2</sub>, releasing the active site on Pd for electrochemical oxidation reaction. The oxide on the surface of the Pd particles could also help to break C-C bond.

PdMn<sub>3</sub>O<sub>4</sub> shows a weaker ethanol oxidation peak compared to that PdNiO. The same observations were reported by Shen et al. [2] where they had found in their study that PdNiO was more active in 1M KOH, 1M ethanol solution when compared to PdMn<sub>3</sub>O<sub>4</sub> on a carbon support material. PdNiO was more active towards ethanol oxidation compared to PdMn<sub>3</sub>O<sub>4</sub> and PdMn<sub>3</sub>O<sub>4</sub>NiO which had current densities lower than that of PdNi, but improved current densities compared to Pd.

The superior catalytic activity for PdNi compared to Pd on a carbon support material observed in this study was in agreement with the results obtained from other studies that compared the two catalysts [3, 4, 5] where the current density was higher for PdNi.



*Table 4.3 Current density values and onset potentials of Pd, PdNi, PdNiO, PdMn<sub>3</sub>O<sub>4</sub> and PdMn<sub>3</sub>O<sub>4</sub>NiO in-house electro-catalysts on MWCNT\_1.0M KOH with 1.0M ethanol at a scan rate of 30mV.s<sup>-1</sup>*

<b>Catalyst</b>	<b>Current density (mAcm<sup>-2</sup>)</b>	<b>Onset potential (V)</b>
<b>Pd</b>	0.20	-0.25
<b>PdNi</b>	0.85	-0.66
<b>PdNiO</b>	2.25	-0.68
<b>PdMn<sub>3</sub>O<sub>4</sub></b>	0.25	-0.18
<b>PdMn<sub>3</sub>O<sub>4</sub>NiO</b>	0.225	-0.90



Figure 4.11 below shows the LSV for the prepared in-house catalysts in glycerol

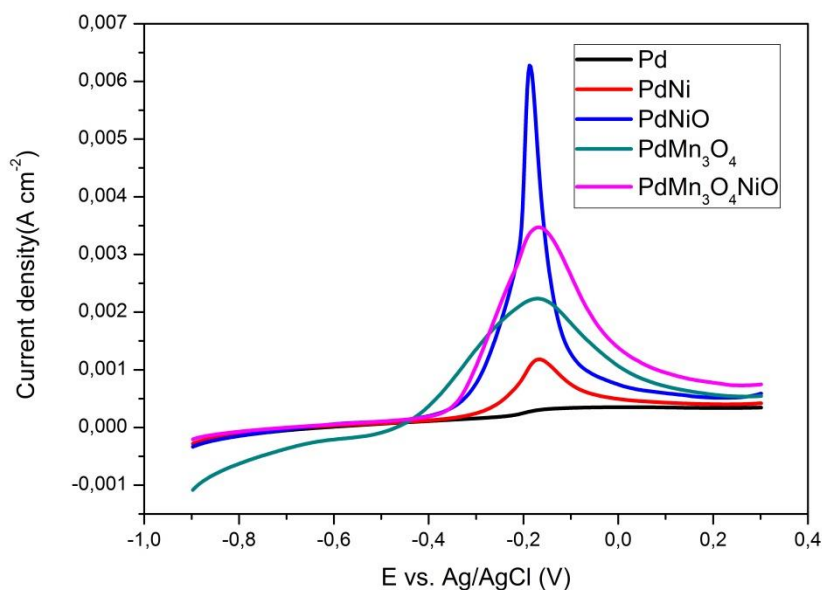


Figure 4.11 Linear sweep voltammetry of Pd, PdNi, PdMn, PdNiO, PdMn<sub>3</sub>O<sub>4</sub> and PdMn<sub>3</sub>O<sub>4</sub>NiO in-house electro-catalysts on MWCNT support in N<sub>2</sub> saturated 1.0M KOH with 1.0M glycerol at a scan rate of 30mV.s<sup>-1</sup>

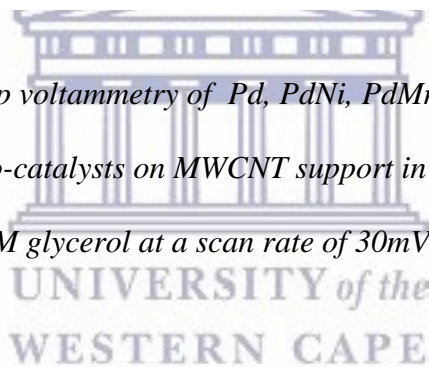


Figure 4.11 shows the combined linear sweep voltammetry of Pd, PdNi, PdNiO, PdMn<sub>3</sub>O<sub>4</sub> and PdMn<sub>3</sub>O<sub>4</sub>NiO in-house electro-catalysts on MWCNT. The LSV's show the glycerol oxidation peaks for the five in-house catalysts. A better alcohol oxidation and more improved current densities are observed compared to those in figure for EOR; see table 4.3 below. The oxides show the best electro.catalytic activity compared to the Pd and PdNi.

In the literature discussed in chapter 2, the activity was expected to improve when another metal was alloyed to the Pd catalyst. All the alloyed catalysts did show an improvement in electrocatalytic activity compared to Pd.

PdNiO again was the most active catalyst with the highest current density and again PdMn<sub>3</sub>O<sub>4</sub> was less active compared to the former like it was observed in figure for EOR. The ternary catalyst PdMn<sub>3</sub>O<sub>4</sub>NiO shows good electro-catalytic activity in glycerol. This could be attributed to the NiO present in the catalyst as it is seen in this study that NiO is a good alloying metal for Pd.

*Table 4.4 Current density values and onset potentials of Pd, PdNi, PdNiO, PdMn<sub>3</sub>O<sub>4</sub> and PdMn<sub>3</sub>O<sub>4</sub>NiO in-house electro-catalysts on MWCNT\_1.0M KOH with 1.0M glycerol at a scan rate of 30mV.s<sup>-1</sup>*

<b>Catalyst</b>	<b>Current density (mAcm<sup>-2</sup>)</b>	<b>Onset potential (V)</b>
<b>Pd</b>	0.35	-0.25
<b>PdNi</b>	1.19	-0.38
<b>PdNiO</b>	6.25	-0.41
<b>PdMn<sub>3</sub>O<sub>4</sub></b>	2.25	-0.51
<b>PdMn<sub>3</sub>O<sub>4</sub>NiO</b>	3.49	-0.39

#### 4.7 Electrochemical impedance spectrometry study

The EIS of the catalysts was studied in order to determine the kinetics of the catalysts. The kinetics was done at two potentials which is -0.3 V and -0.1V

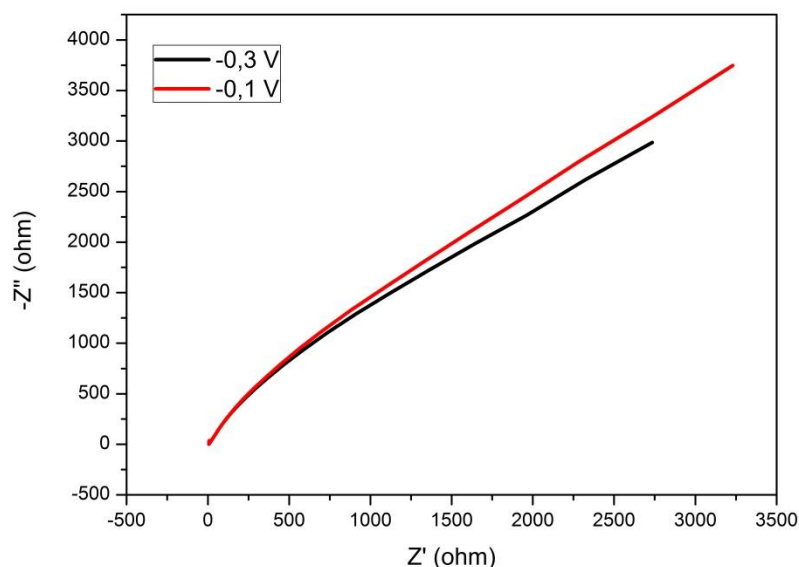
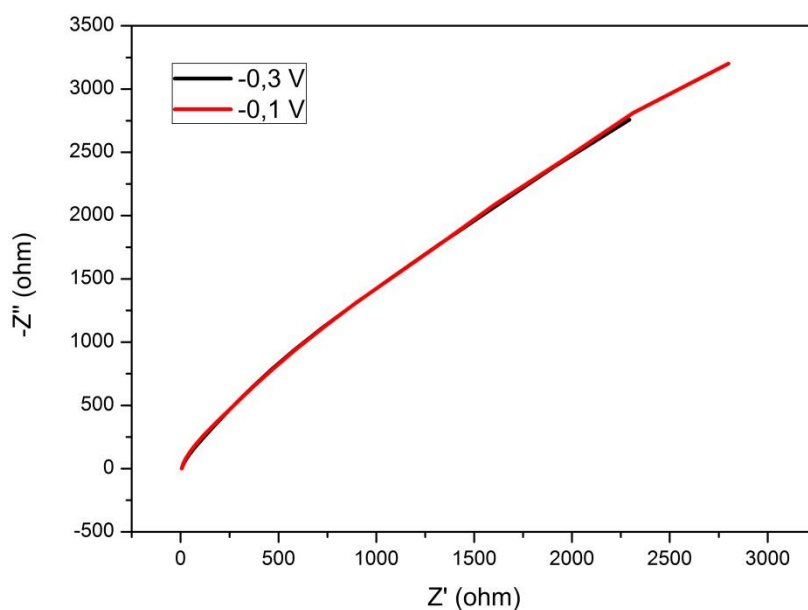


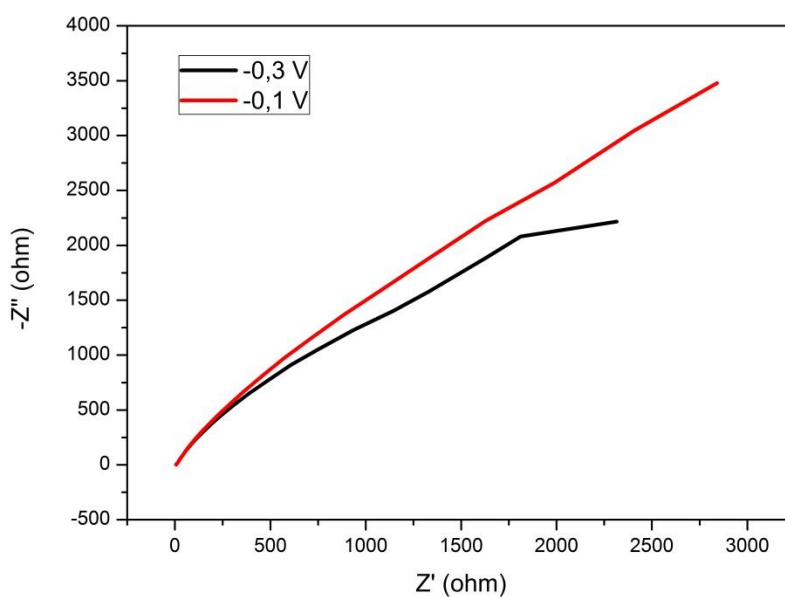
Figure 4.12 Impedance of Pd in-house electro-catalysts on MWCNT support in  $N_2$  saturated 1.0M KOH comparing the activity in 1M ethanol at -0.1V and -0.3V

Figure 4.12 shows the impedance of Pd on MWCNTs as a support material in 1M KOH with 1M ethanol at two different potentials. From the figure above it shows that the electrode kinetics after alcohol oxidation are slower than before oxidation. The EIS for onset potential and alcohol oxidation show a linear trend, but a lower slope is observed for the onset potential.



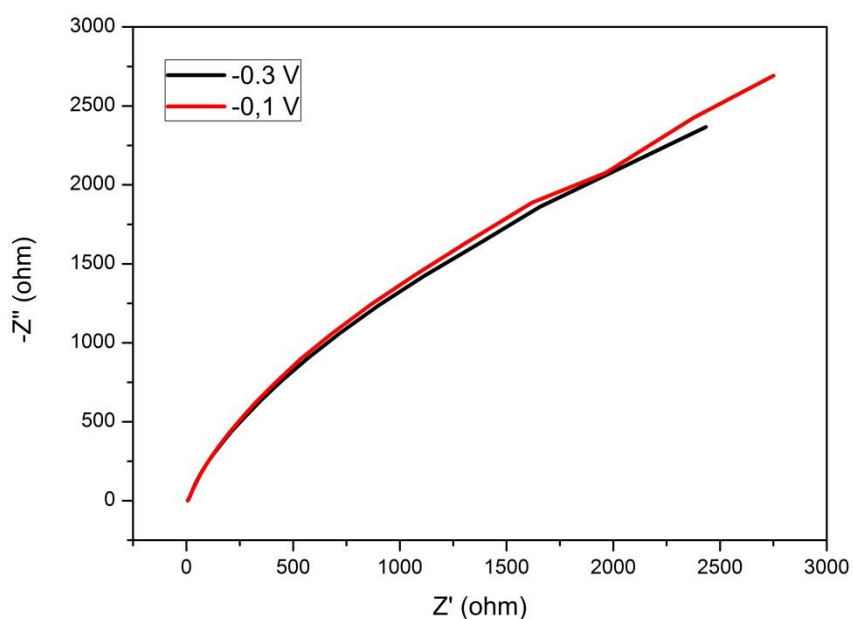
*Figure 4.13 Impedance of Pd in-house electro-catalysts on MWCNT support in N<sub>2</sub> saturated 1.0M KOH comparing the activity in 1M glycerol at -0.1V and -0.3V.*

Figure 4.13 shows the impedance of Pd on MWCNTs as a support material in 1M KOH with 1M glycerol at two different potentials. From the figure it is seen that the electrode kinetics for the onset potential and after the alcohol oxidation was the same for the catalyst. The catalysts shows a linear trend at both potentials.



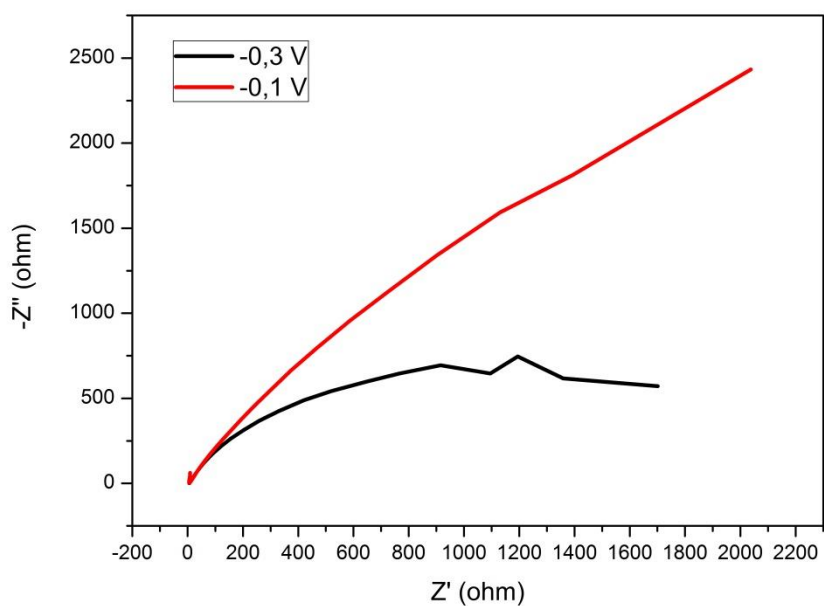
*Figure 4.14 Impedance of PdNi in-house electro-catalysts on MWCNT support in  $N_2$  saturated 1.0M KOH comparing the activity in 1M ethanol at -0.1V and -0.3V.*

Figure 4.14 shows the impedance of PdNi on MWCNTs as a support material in 1M KOH with 1M ethanol at two different potentials. The electrode kinetics after alcohol oxidation are slower than that before alcohol oxidation. The EIS for onset potential shows a linear trend but which is not as steep as the one observed after alcohol oxidation.



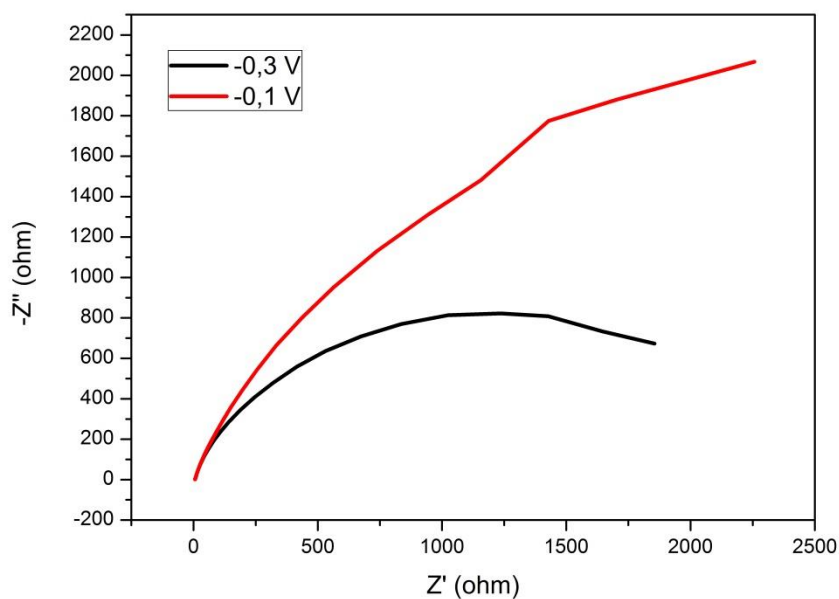
*Figure 4.15 Impedance of PdNi in-house electro-catalysts on MWCNT support in  $N_2$  saturated 1.0M KOH comparing the activity in 1M glycerol at -0.1V and -0.3V.*

Figure 4.15 shows the impedance observed for PdNi on MWCNTs on MWCNTs as a support material in 1M KOH with 1M glycerol at two different potentials. The figure shows a linear trend is observed for electrode kinetics before and after alcohol oxidation.



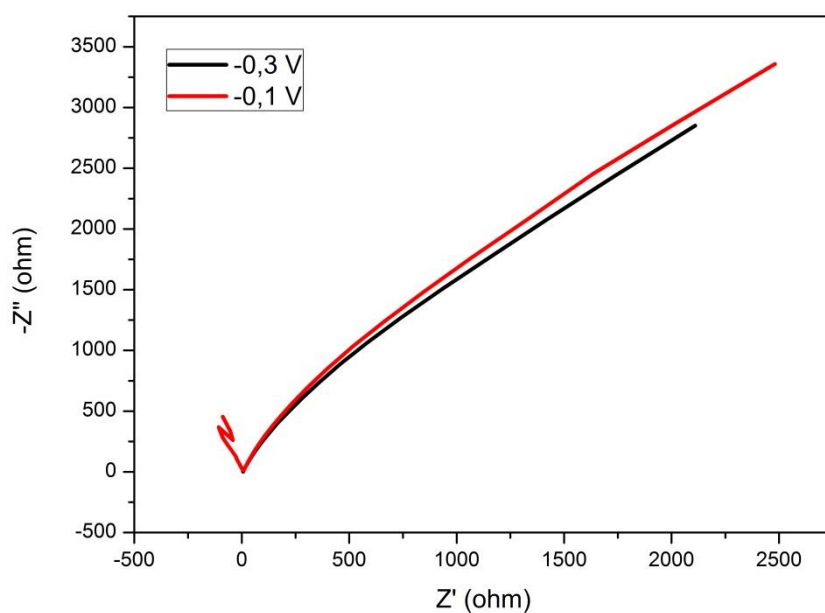
*Figure 4.16 Impedance of PdNiO in-house electro-catalysts on MWCNT support in N<sub>2</sub> saturated 1.0M KOH comparing the activity in 1M ethanol at -0.1V and -0.3V.*

Figure 4.16 shows the impedance observed for PdNiO on MWCNTs as a support material in 1M KOH with 1M ethanol at two different potentials. From the figure above, the electrode kinetics before oxidation are faster than after oxidation. The EIS for onset potential shows semi-circle while a linear trend is observed after alcohol oxidation.



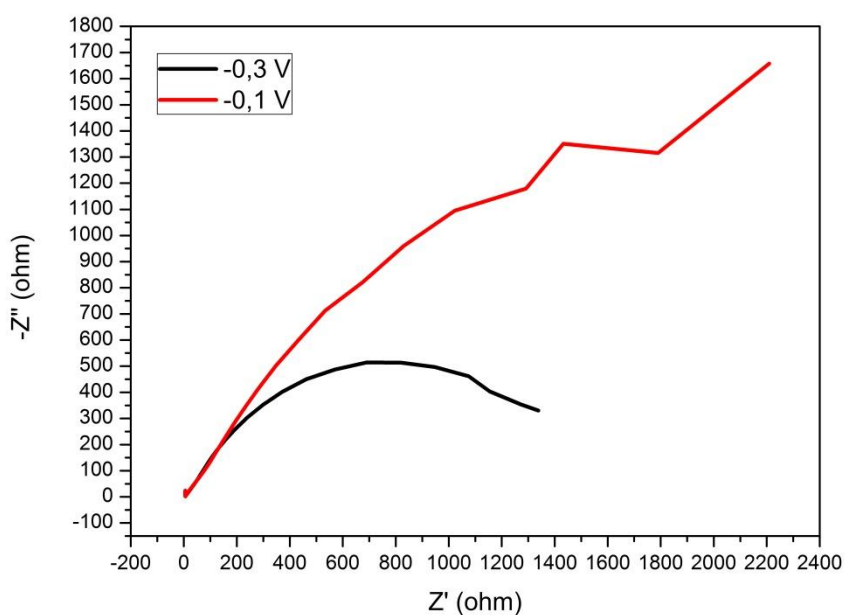
*Figure 4.17 Impedance of PdNiO in-house electro-catalysts on MWCNT support in N<sub>2</sub> saturated 1.0M KOH comparing the activity in 1M glycerol at -0.1V and -0.3V.*

Figure 4.17 shows the impedance observed for PdNiO on MWCNTs as a support material in 1M KOH with 1M glycerol at two different potentials. The figure above clearly shows that the electrode kinetics before oxidation are faster than after oxidation. The EIS onset potential shows a semi-circle, while after alcohol oxidation a linear trend is observed.



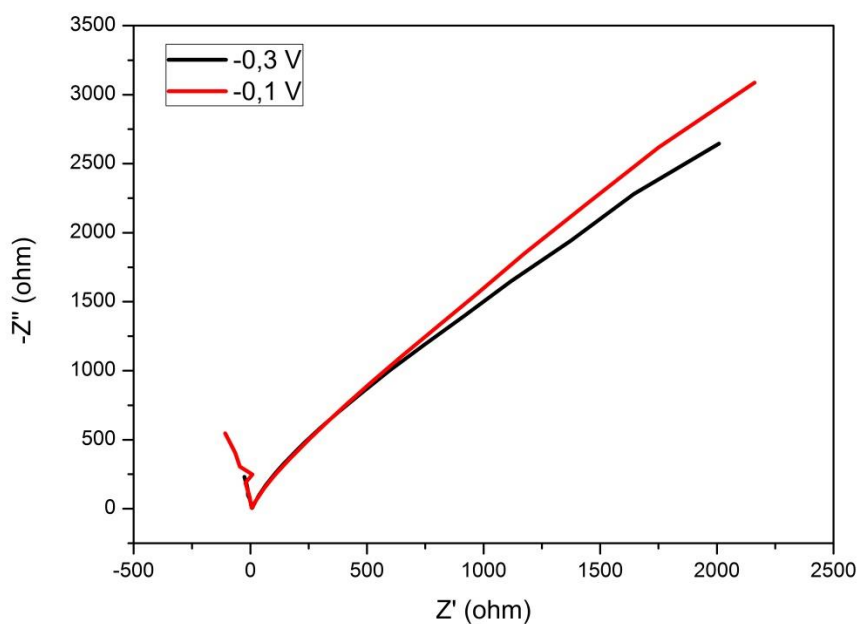
*Figure 4.18 Impedance of PdMn<sub>3</sub>O<sub>4</sub> in-house electro-catalysts on MWCNT support in N<sub>2</sub> saturated 1.0M KOH comparing the activity in 1M ethanol at -0.1V and -0.3V.*

Figure 4.18 shows the impedance observed for PdMn<sub>3</sub>O<sub>4</sub> ON MWCNTs as a support material in 1M KOH with 1M ethanol at two different potentials. From the figure above, the electrode kinetics before and after oxidation both follow a linear trend. The linear trend after alcohol oxidation has a slightly steeper slope. So the electrode kinetics at -0.3 V are faster than those at -0.1 V.



*Figure 4.19 Impedance of PdMn<sub>3</sub>O<sub>4</sub> in-house electro-catalysts on MWCNT support in N<sub>2</sub> saturated 1.0M KOH comparing the activity in 1M glycerol at -0.1V and -0.3V.*

Figure 4.19 shows the impedance observed for PdMn<sub>3</sub>O<sub>4</sub> on MWCNTs as a support material in 1M KOH with 1M glycerol at two different potentials. The figure clearly shows that the electrode kinetics before oxidation is faster than after oxidation. The EIS for onset potential shows semi-circle while after oxidation a linear trend is observed.



*Figure 4.20 Impedance of PdMn<sub>3</sub>O<sub>4</sub>NiO in-house electro-catalysts on MWCNT support in N<sub>2</sub> saturated 1.0M KOH comparing the activity in 1M ethanol at -0.1V and -0.3V.*

Figure 4.20 shows the impedance observed for PdMn<sub>3</sub>O<sub>4</sub>NiO on MWCNTs as a support material in 1M KOH with 1M ethanol at two different potentials. The figure above shows that the electrode kinetics at -0.3 V are faster than at -0.1 V. The EIS onset potential shows a less steep slope compared to that after alcohol oxidation.

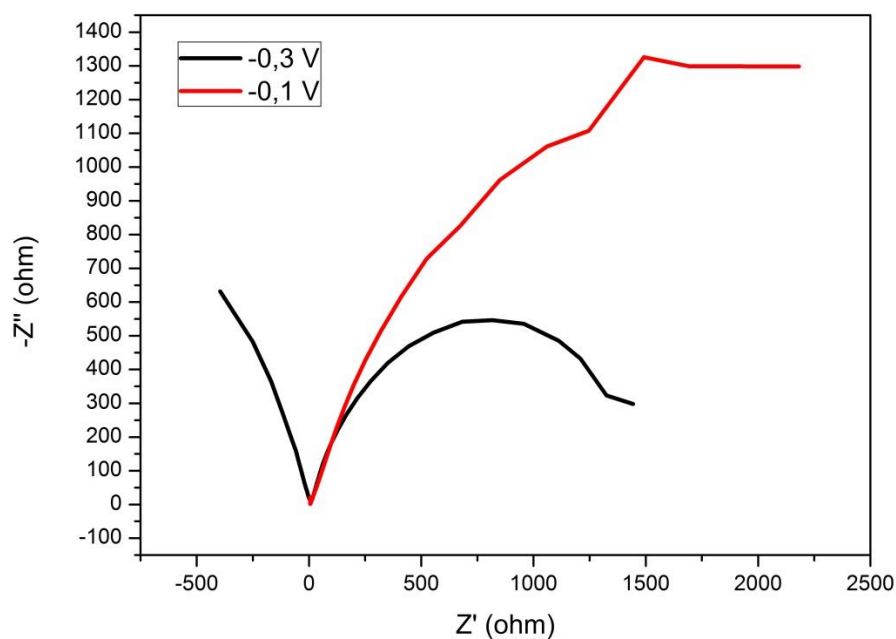


Figure 4.21 Impedance of  $\text{PdMn}_3\text{O}_4\text{NiO}$  in-house electro-catalysts on MWCNT support in  $\text{N}_2$  saturated 1.0M KOH comparing the activity in 1M glycerol at -0.1V and -0.3V.

Figure 4.21 shows the impedance observed for  $\text{PdMn}_3\text{O}_4\text{NiO}$  on MWCNTs as a support material in 1M KOH with 1M glycerol at two different potentials. The figure above shows that electrode kinetics before oxidation are clearly faster than after oxidation. The EIS for onset potential shows semi-circle while after alcohol oxidation a linear trend is observed.

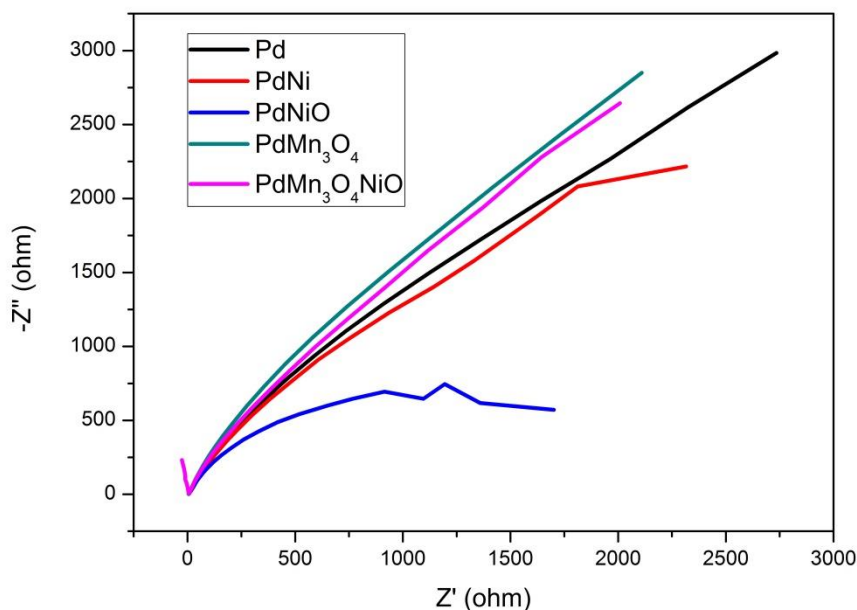
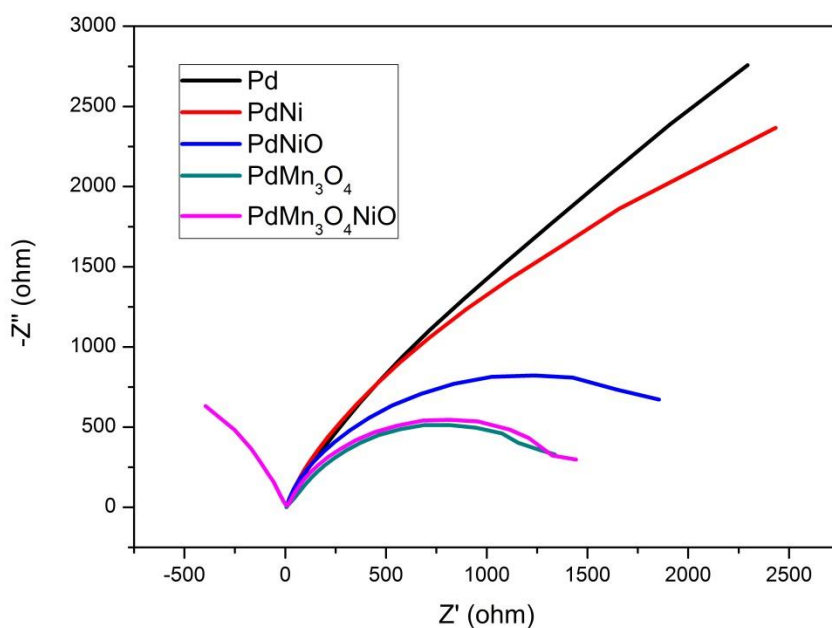


Figure 4.22 Impedance of Pd, PdNi, PdMn, PdNiO, PdMn<sub>3</sub>O<sub>4</sub> and PdMn<sub>3</sub>O<sub>4</sub>NiO in-house electro-catalysts on MWCNT support in N<sub>2</sub> saturated 1.0M KOH comparing the activity in 1M ethanol at -0.3V

From the impedance spectra in figure 4.22 it is observed that the electrode kinetics for the two most active catalysts in ethanol, PdNiO and PdNi were faster in the same alcohol. Nickel alloyed Pd catalysts towards ethanol oxidation in this study show that their kinetics are faster compared to Pd alloyed Mn<sub>3</sub>O<sub>4</sub> based oxides. Results obtained for PdMn<sub>3</sub>O<sub>4</sub>NiO and PdMn<sub>3</sub>O<sub>4</sub> validate the results obtained in LSV studies that NiO based catalysts are more active towards Ethanol compared to Mn<sub>3</sub>O<sub>4</sub> based Pd catalysts. The mono-catalyst Pd showed better performance in terms of kinetics than the Mn<sub>3</sub>O<sub>4</sub> catalysts.



*Figure 4.23 Impedance of Pd, PdNi, PdMn, PdNiO, PdMn<sub>3</sub>O<sub>4</sub> and PdMn<sub>3</sub>O<sub>4</sub>NiO in-house electro-catalysts on MWCNT support in N<sub>2</sub> saturated 1.0M KOH comparing the activity in 1M glycerol at -0.3V*

The impedance spectra of in figure 4.23 shows that the best electrode kinetics is for the catalysts which are binary with metal oxides. These were the expected results where metal oxides would improve the performance of the Pd electro-catalyst. The mono catalyst was the least performing catalyst, where even the kinetics for PdNi was faster. Employing a second catalyst clearly improves kinetics of a catalyst in glycerol.

## 4.8 Chronoamperometry study

Chronoamperometry was done in order to compare the stability of the catalysts.

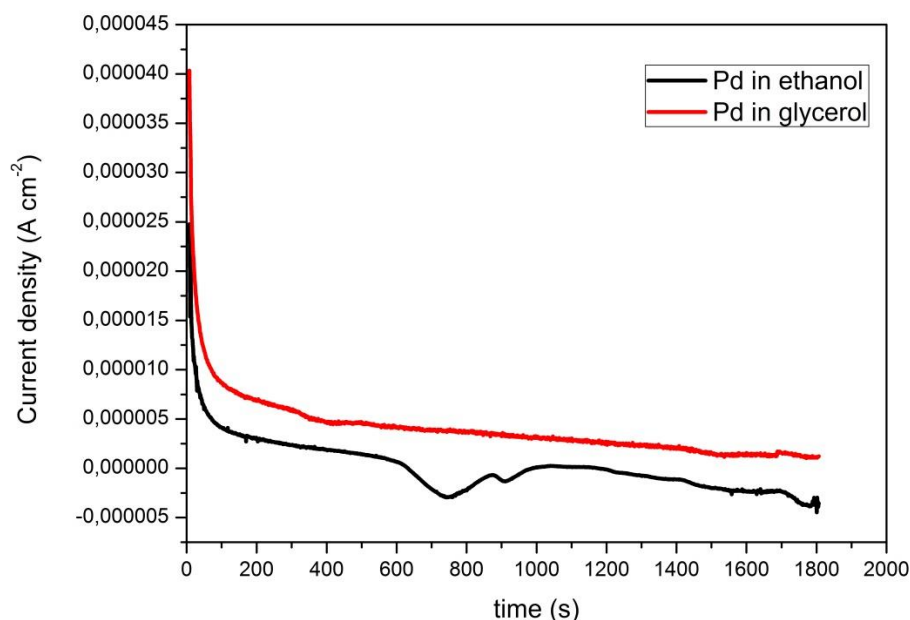
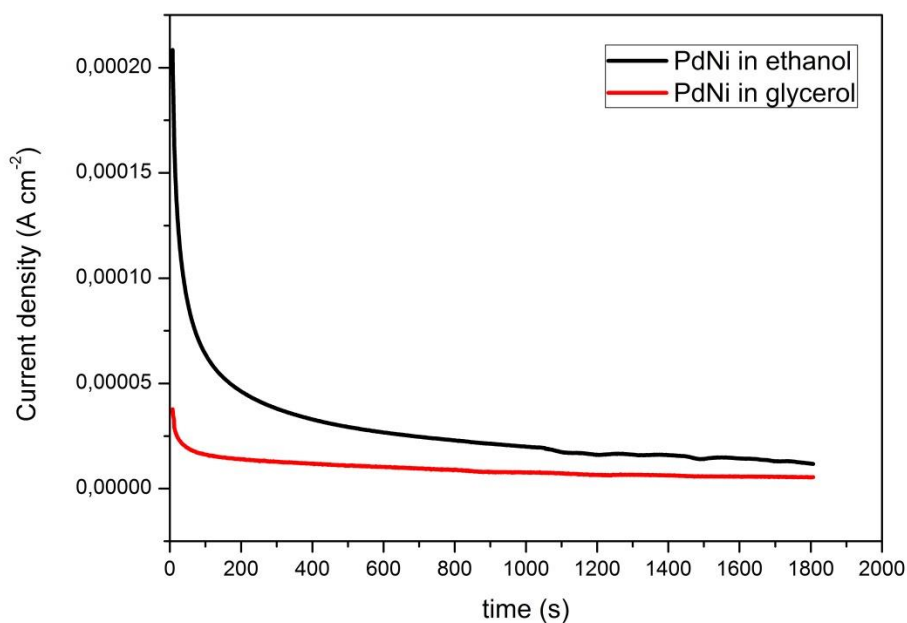


Figure 4.24 Chronoamperometry of Pd in-house electro-catalysts on MWCNT support in  $N_2$  saturated 1.0M KOH comparing the stability in 1M ethanol and 1M glycerol at a -0.2V

Figure 4.24 shows chronoamperometry of Pd in house catalyst on MWCNTs support in nitrogen saturated 1M KOH, comparing the stability in 1M ethanol and 1M glycerol at -0.2 V. As we observed for LSV data, the catalyst gave higher current density in glycerol when compared to ethanol. The Pd catalyst had its current density drop to  $3\mu\text{Acm}^{-2}$  in glycerol; however it was less stable in ethanol with the current density dropping even lower to  $-3\mu\text{Acm}^{-2}$ . The higher current density exhibited in exhibited by Pd for glycerol shows better oxidation compared to ethanol. The results collaborate with those in figure for linear sweep voltammetry.



*Figure 4.25 Chronoamperometry of PdNi in-house electro-catalysts on MWCNT support in N<sub>2</sub> saturated 1.0M KOH comparing the stability in 1M ethanol and 1M glycerol at -0.2V.*

Figure 4.25 shows chronoamperometry of PdNi in house catalyst on MWCNTs support in nitrogen saturated 1M KOH comparing the stability in 1M ethanol and 1M glycerol at -0.2 V. the PdNi catalyst shows better stability in ethanol compared to glycerol. A higher current density was observed for ethanol at 12.5  $\mu\text{Acm}^{-2}$  and glycerol had a current density of 6  $\mu\text{Acm}^{-2}$  after 1800 s.















